AIMS Mathematics, 11(4): 11116–11153.
DOI: 10.3934/math.2026458
Received: 10 March 2026
Revised: 07 April 2026
Accepted: 15 April 2026
Published: 21 April 2026

http://www.aimspress.com/journal/Math

*Research article*

# Modeling Guinea worm disease with time delays: Threshold dynamics, treatments and sensitivity analysis in heterogeneous populations

**Fawaz K. Alalhareth[1,2,*], Ali A. Alharbi[3], Mohammed H. Alharbi[3] and Miled El Hajji[3,4]**

[1] Department of Mathematics, College of Arts and Sciences, Najran University, Najran, Saudi Arabia
[2] Science and Engineering Research Center, Najran University, Najran, Saudi Arabia
[3] Department of Mathematics and Statistics, Faculty of Science, University of Jeddah, P.O. Box 80327, Jeddah 21589, Saudi Arabia
[4] ENIT-LAMSIN, BP. 37, 1002 Tunis-Belvédère, Tunis El Manar University, Tunisia

* **Correspondence:** Email: fkalalhareth@nu.edu.sa.

**Abstract:** This paper presents a mathematical investigation of Guinea worm disease (GWD) dynamics using a two-patch model that incorporates discrete delays and treatment interventions. The model accounts for two distinct host populations sharing a common water source, with dynamics described by a system of delay differential equations. We compute the basic reproduction number $\mathscr{R}_0^d$ for both the delayed and nondelayed systems and establish threshold conditions for disease eradication and persistence. Analytical results demonstrate that the disease-free equilibrium is globally asymptotically stable (GAS) when $\mathscr{R}_0^d \leq 1$, while a unique endemic equilibrium exists and is globally stable when $\mathscr{R}_0^d > 1$. Sensitivity analysis identifies key parameters influencing disease transmission, and numerical simulations explore the impact of time delays and treatment efficacy on disease dynamics. Our findings reveal that both treatment interventions and specific time delays can significantly reduce the basic reproduction number, providing valuable insights for designing effective GWD control strategies.

**Keywords:** Guinea worm disease; delay differential equations; global stability; treatment interventions; sensitivity analysis; mathematical modeling
**Mathematics Subject Classification:** 34D23, 92D30, 92B05, 37N25

## 1. Introduction

Over the past three decades, the global community has witnessed a substantial decline in Guinea worm disease (GWD) cases, from an estimated 3.5 million across 20 countries in 1986 to merely 22 cases reported in 2015, confined to just four nations: South Sudan, Mali, Chad, and Ethiopia [1].

This remarkable achievement is widely credited to the Guinea Worm Eradication Program launched in the 1980s [1, 2]. Despite this progress, several persistent challenges threaten global eradication efforts. A significant obstacle is the continued reliance on and sharing of untreated open water sources by diverse communities in endemic regions, where differential knowledge and behaviors regarding the disease exist [1, 3, 4]. These heterogeneities critically influence GWD dynamics and necessitate a thorough evaluation of eradication prospects under such conditions. The recent emergence of new epidemiological challenges has further complicated eradication efforts. Notably, the discovery of GWD infections in animal hosts, particularly domestic dogs in Chad, has introduced a previously unrecognized reservoir that could sustain transmission even after human cases are eliminated [2]. This zoonotic transmission pathway represents a significant threat to eradication, as it creates an environmental reservoir that can reignite human outbreaks. Additionally, civil unrest, population displacement, and limited healthcare infrastructure in remaining endemic areas continue to hamper surveillance and intervention efforts, allowing the disease to persist in hard-to-reach communities.

GWD is a debilitating waterborne parasitic infection caused by *Dracunculus medinensis*. Humans contract the disease by drinking water contaminated with copepods (small crustaceans) harboring the parasite's infective larvae [1, 5]. The complex lifecycle involves multiple biological stages, each with distinct temporal characteristics that are crucial for understanding transmission dynamics. After ingestion, the larvae are released, mature, and migrate within the host, with the female worm eventually emerging through a painful blister on the skin, often on the lower extremities [6]. This emergence process typically occurs approximately one year after infection, representing a significant delay in the manifestation of infectiousness. The intense discomfort prompts individuals to immerse the affected area in water, which stimulates the release of thousands of new larvae into the environment, thereby completing the transmission cycle when these larvae are ingested by copepods [7]. The extended temporal nature of the Guinea worm lifecycle, characterized by multiple developmental delays both within the human host and in the aquatic environment, creates unique challenges for disease modeling and control. The parasite must survive through various stages: the incubation period in humans, the maturation period in copepods, and the free-living larval stage in water. Each of these stages has distinct mortality risks and temporal durations that collectively determine the overall transmission potential. Although mortality is rare, the disease can cause permanent disability, economic loss, and school absenteeism [8, 9], with significant impacts on agricultural productivity and community welfare in already vulnerable populations.

In the absence of a vaccine or drug therapy, the eradication strategy relies exclusively on preventive measures. These include providing safe water sources, promoting water filtration, delivering health education, applying the larvicide Abate (temephos), and ensuring strict case containment to prevent water source contamination [10–12]. The effectiveness of these interventions is highly dependent on community compliance, which in turn is influenced by cultural practices, economic constraints, and the perceived severity of the disease threat. The temporal aspect of interventions is particularly crucial, as the effects of educational campaigns may wane over time, and seasonal variations in water source usage can dramatically alter transmission patterns.

Mathematical modeling serves as a powerful tool for understanding complex biological phenomena that are difficult to measure directly in the field [13–15]. By capturing the essential features of disease transmission through mathematical formalism, models can identify key leverage points for intervention, predict the long-term impact of control strategies, and optimize resource allocation in

elimination campaigns. While several mathematical models have been developed for GWD [16–18], they have not comprehensively explored the impact of time-dependent educational campaigns on long-term disease dynamics in a heterogeneous setting where multiple communities share a common water source. Furthermore, existing models often neglect the critical temporal delays inherent in the parasite's lifecycle, which may significantly alter predictions about intervention effectiveness and eradication timelines. Recent advances in delay differential equation models have been applied to various ecological and epidemiological systems, including predator–prey dynamics with stage structure and anti-predator behavior [19], as well as delayed diffusive models incorporating memory-based diffusion and fear effects [20], demonstrating the versatility of delay formulations in capturing complex biological interactions. The literature on epidemic models that couple disease spread with information dissemination is also substantial [21–23]. For instance, [24] used a deterministic model to show how time-dependent education lowers susceptibility, and [21] illustrated the effect of media awareness on outbreak dynamics. These studies demonstrate that behavioral changes driven by disease awareness can fundamentally alter transmission dynamics, creating feedback loops between infection prevalence and protective behaviors. However, the application of these modeling approaches to GWD remains limited, particularly in addressing the unique challenges posed by its environmental transmission pathway and extended temporal dynamics.

In recent years, mathematical modeling of GWD has advanced considerably, particularly following the recognition that dogs can serve as reservoir hosts for *Dracunculus medinensis* [2]. Early models focused primarily on human-copepod transmission dynamics, including the foundational work of Netshikweta and Garira [25], who proposed a multiscale model suggesting that water source treatment is the most effective control strategy. A major advancement came with the incorporation of zoonotic transmission. Helikumi and Mushayabasa [26] refined compartmental models including both human and dog populations, distinguishing between free-ranging and non-free-ranging dogs, demonstrating that elimination requires targeting both populations. Mushayabasa, Losio, Modnak, and Wang [27] applied optimal control theory to a two-patch GWD model with different host populations sharing a common water source, exploring time-dependent education campaigns for disease elimination within 120 months. Losio and Mushayabasa [18] investigated the effects of spatial heterogeneity and seasonality on GWD transmission. Most recently, Lusekelo et al. [28] developed a nonautonomous model incorporating seasonality and heterogeneous mean worm burden in dog populations, revealing that seasonal fluctuations in fishing activities significantly influence disease prevalence. Smalley et al. [29] utilized agent-based simulation to analyze proactive tethering strategies for dogs in Chad, demonstrating that intervention timing and dog selection critically impact eradication outcomes. Despite these advances, existing models have not comprehensively explored the impact of multiple discrete biological time lags—representing latent periods in humans, maturation within hosts, and environmental development in copepods—on GWD transmission dynamics in heterogeneous populations sharing a common water source.

The model presented in this paper offers several novel features that distinguish it from existing GWD models. First, while most existing models neglect explicit biological time lags or use only simple delays, our model incorporates five discrete delays ($\iota_1$ to $\iota_5$) capturing distinct stages: the time between water consumption and establishment of latent infection ($\iota_1, \iota_3$), the maturation period from latent to infectious stages ($\iota_2, \iota_4$), and the environmental development time of larvae within copepods ($\iota_5$). Second, unlike single-population or basic two-patch models without explicit stage-

specific delays, our model features a two-patch structure with heterogeneous communities differing in awareness, infection risk ($\beta_1 \neq \beta_2$), and behaviors, all sharing a common water source. Third, whereas previous models typically employ either exposed compartments *or* delays, our model uses a dual representation where exposed compartments ($E_1, E_2$) track current latent individuals while delays capture fixed progression durations with stage-specific mortality (via exponential survival probabilities $e^{-m_i \iota_i}$). Fourth, while existing work often provides only local stability analysis or basic reproduction number calculations, we present global asymptotic stability proofs using Lyapunov functionals for both disease-free and endemic equilibria under delayed dynamics. Fifth, we introduce a treatment efficacy parameter $\kappa$ with an explicit critical threshold $\kappa^{\text{cr}} = 1 - 1/\mathscr{R}_0^d$ for disease eradication, and we perform a comprehensive sensitivity analysis identifying the environmental delay $\iota_5$ as the most influential. These innovations provide quantitative, actionable public health guidance for Guinea worm eradication efforts.

This paper is organized as follows: Section 2 presents the formulation of a two-patch delayed differential equation model, including biological justification for state variables, parameters, and the incorporation of multiple discrete delays; Section 3 defines and proves the biologically feasible domain, derives the basic reproduction number $\mathscr{R}_0$, establishes existence conditions for equilibria, and uses Lyapunov functions to prove global stability of disease-free and endemic equilibria; Section 4 extends invariance results to the delayed model, derives the delayed reproduction number $\mathscr{R}_0^d$, analyzes equilibria, and proves global stability using Lyapunov functionals that incorporate delays; Section 5 provides a numerical verification of theoretical stability results using MATLAB, a sensitivity analysis of $\mathscr{R}_0^d$ using normalized forward sensitivity indices, analyzes how treatment efficacy affects disease dynamics and identifies critical thresholds, and finally examines how developmental delays influence disease persistence and control; finally, Section 6 summarizes key findings, discusses limitations of the study, and suggests directions for future research. This structure progresses systematically from model development through theoretical analysis to numerical verification, providing a comprehensive investigation of Guinea worm disease dynamics with discrete delays and control interventions.

## 2. Derivation of the mathematical model

We developed a two-patch mathematical model for Guinea worm disease (GWD) to simulate a scenario where two distinct human populations share a common water source. The patches are differentiated by their level of GWD awareness, which influences their infection risk and contribution to environmental pathogen load [1]. This structure is inspired by rural endemic regions like Ethiopia, where only 42 out of 70 villages have access to potable water [30], forcing communities to share untreated open water sources [4]. As highlighted by [3], heterogeneity in health education is a key socioeconomic driver of differential infection risks. The proposed model extends the work of [27] by incorporating several discrete delays.

The delayed model (2.1) captures the complex biological lifecycle of GWD transmission. Susceptible individuals ($S_1$, $S_2$) become infected by consuming water containing infectious copepods ($I_c$) carrying Guinea worm larvae, with infection terms $\beta_1 S_1 I_c$ and $\beta_2 S_2 I_c$. The discrete delays account for key biological processes: $\iota_1$ and $\iota_3$ represent the time between water consumption and establishment of latent infection, with survival probabilities $e^{-m_1 \iota_1}$ and $e^{-m_3 \iota_3}$. The transitions from latent to infectious stages ($I_1$, $I_2$) occur after additional delays $\iota_2$ and $\iota_4$, with survival

probabilities $e^{-m_2\iota_2}$ and $e^{-m_4\iota_4}$. Environmental contamination by actively infectious individuals occurs after delay $\iota_5$, representing larval development within copepods, with survival probability $e^{-m_5\iota_5}$. This two-patch structure acknowledges heterogeneous communities with different infection risks ($\beta_1 \neq \beta_2$), awareness levels, and behaviors, all sharing a common water reservoir. Figure 1 presents the transmission diagram.

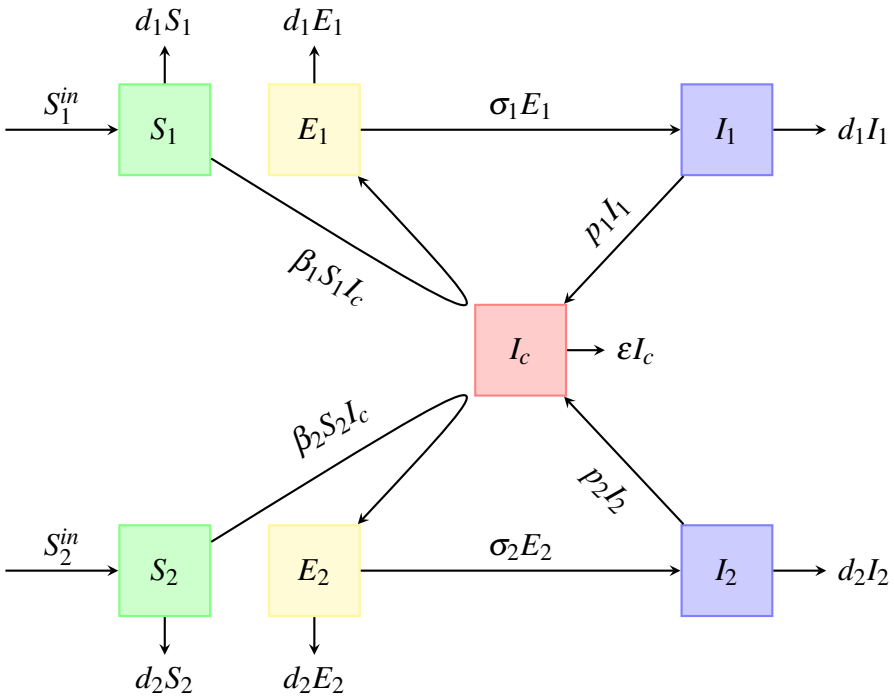


**Figure 1.** Guinea worm disease transmission diagram.

This model represents a two-patch system where two distinct human populations share a common water source contaminated with Guinea worm larvae. The state variables are defined as follows: $S_1$ and $S_2$ represent susceptible individuals in patches 1 and 2 respectively; $E_1$ and $E_2$ denote latently infected individuals; $I_1$ and $I_2$ represent actively infected individuals; and $I_c$ represents the concentration of infectious larvae in the shared water source. The system incorporates five discrete delays ($\iota_1$ to $\iota_5$) that account for various biological time lags in the disease transmission cycle, including the latent period within human hosts and development times in the environment. The exponential terms $e^{-m_i\iota_i}$ represent survival probabilities over these delay periods, where $m_i$ are delay decay parameters. The model parameters include recruitment rates $S_1^{in}$ and $S_2^{in}$, natural mortality rates $d_1$ and $d_2$, infection rates $\beta_1$ and $\beta_2$, progression rates $\sigma_1$ and $\sigma_2$, shedding rates $p_1$ and $p_2$, and pathogen decay rate $\varepsilon$. A summary of the biological interpretation of state variables and parameters is given in Table 1.

**Table 1.** Biological interpretation of state variables and parameters.

| | |
|---|---|
| $S_1$ | Number of susceptible individuals in Patch 1 (lower-awareness community) |
| $E_1$ | Number of latently infected individuals in Patch 1 (infected but not yet infectious) |
| $I_1$ | Number of actively infected (infectious) individuals in Patch 1 |
| $S_2$ | Number of susceptible individuals in Patch 2 (higher-awareness community) |
| $E_2$ | Number of latently infected individuals in Patch 2 |
| $I_2$ | Number of actively infected (infectious) individuals in Patch 2 |
| $I_c$ | Concentration of infectious *Dracunculus medinensis* larvae in the shared water source |
| $S_1^{in}$ | Recruitment level—the total (target) population size in patch 1 |
| $S_2^{in}$ | Recruitment level—the total (target) population size in patch 2 |
| $d_1$ | Natural mortality rate for individuals in Patch 1 |
| $d_2$ | Natural mortality rate for individuals in Patch 2 |
| $\beta_1$ | Transmission rate from contaminated water to susceptible individuals in Patch 1 |
| $\beta_2$ | Transmission rate from contaminated water to susceptible individuals in Patch 2 |
| $\sigma_1$ | Progression rate from latent stage ($E_1$) to infectious stage ($I_1$) in Patch 1 |
| $\sigma_2$ | Progression rate from latent stage ($E_2$) to infectious stage ($I_2$) in Patch 2 |
| $p_1$ | Shedding rate of larvae into water from infectious individuals in Patch 1 |
| $p_2$ | Shedding rate of larvae into water from infectious individuals in Patch 2 |
| $\varepsilon$ | Decay rate of infectious larvae in the water source (natural mortality + filtration effects) |
| $\iota_1, \iota_3$ | Discrete delay representing time between water consumption and establishment of latent infection in Patch 1 and Patch 2, respectively |
| $\iota_2, \iota_4$ | Discrete delay representing maturation period from latent to infectious stage within human hosts in Patch 1 and Patch 2, respectively |
| $\iota_5$ | Discrete delay representing development time of larvae into infectious forms within copepods in the aquatic environment |
| $m_i$ | Delay decay (mortality) rates during the respective delay periods; the exponential factor $e^{-m_i\iota_i}$ represents the survival probability over delay $\iota_i$ |
| $\kappa$ | Treatment efficacy parameter, reducing effective transmission rates by a factor $(1-\kappa)$ |

The dynamical system governing the Guinea worm disease transmission is described by the following system of delay differential equations (DDEs):

$$\begin{cases} \dot{S}_1 &= S_1^{in} - d_1 S_1 - \beta_1 S_1 I_c, \\ \dot{E}_1 &= \beta_1 e^{-m_1\iota_1} S_1(t-\iota_1) I_c(t-\iota_1) - (d_1+\sigma_1)E_1, \\ \dot{I}_1 &= \sigma_1 e^{-m_2\iota_2} E_1(t-\iota_2) - d_1 I_1, \\ \dot{S}_2 &= S_2^{in} - d_2 S_2 - \beta_2 S_2 I_c, \\ \dot{E}_2 &= \beta_2 e^{-m_3\iota_3} S_2(t-\iota_3) I_c(t-\iota_3) - (d_2+\sigma_2)E_2, \\ \dot{I}_2 &= \sigma_2 e^{-m_4\iota_4} E_2(t-\iota_4) - d_2 I_2, \\ \dot{I}_c &= e^{-m_5\iota_5}[p_1 I_1(t-\iota_5) + p_2 I_2(t-\iota_5)] - \varepsilon I_c. \end{cases} \tag{2.1}$$

Whereas the exposed compartments $E_1$ and $E_2$ track the number of individuals currently in the latent stage, the discrete delays $\iota_1$ and $\iota_3$ represent the fixed duration between exposure and the onset of latency, and $\iota_2$ and $\iota_4$ represent the duration between latency onset and infectiousness. This dual

representation allows us to incorporate stage-specific mortality (via the exponential factors) and to account for variability in progression times through the exposed compartment dynamics.

The initial values of the dynamical system (2.1) are given by

$$(S_1,E_1,I_1,S_2,E_2,I_2,I_c)(\theta)=(\varphi_1,\varphi_2,\varphi_3,\varphi_4,\varphi_5,\varphi_6,\varphi_7)(\theta),\varphi_i(\theta)\geq 0,i=1,\cdots,7,\quad \theta\in[-\iota^{max},0],$$

with $\iota^{max}=\max\{\iota_1,\iota_2,\iota_3,\iota_4,\iota_5\}$, $\varphi_i\in C([-\iota^{max},0],\mathbb{R}_+)$, and $C:[-\iota^{max},0]\longrightarrow\mathbb{R}_+$ is the Banach space of continuous functions associated with the norm $\|\varphi_i\|=\sup_{-\iota^{max}\leq\theta\leq 0}|\varphi_i(\theta)|$ for $\varphi_i\in C$, and $i=1,\cdots,7$.

Next, we will start by examining the simplified version of the Guinea worm disease model by neglecting discrete delays, and we will provide a foundational analysis of the model's dynamics.

## 3. Analysis of the nondelayed model

This section examines the simplified version of the Guinea worm disease model without discrete delays, providing a foundational analysis of the system's dynamics. We begin by establishing the biologically feasible region and proving its positive invariance. The basic reproduction number $\mathscr{R}_0$ is derived, and threshold conditions for the existence and stability of equilibria are established. Specifically, we show that the disease-free equilibrium is globally asymptotically stable when $\mathscr{R}_0\leq 1$, while a unique endemic equilibrium exists and is globally stable when $\mathscr{R}_0>1$. These results serve as a benchmark for comparing the effects of delays introduced later in the study.

$$\begin{cases}\dot{S}_1=S_1^{in}-\beta_1S_1I_c-d_1S_1,\\ \dot{E}_1=\beta_1S_1I_c-(\sigma_1+d_1)E_1,\\ \dot{I}_1=\sigma_1E_1-d_1I_1,\\ \dot{S}_2=S_2^{in}-\beta_2S_2I_c-d_2S_2,\\ \dot{E}_2=\beta_2S_2I_c-(\sigma_2+d_2)E_2,\\ \dot{I}_2=\sigma_2E_2-d_2I_2,\\ \dot{I}_c=p_1I_1+p_2I_2-\varepsilon I_c,\end{cases}\tag{3.1}$$

with initial condition $(S_1^0,E_1^0,I_1^0,S_2^0,E_2^0,I_2^0,I_c^0)\in\mathbb{R}_+^7$ . The nondelayed version of the Guinea worm model (3.1) follows an SEI-type (Susceptible-Exposed-Infected type) structure for each patch, with compartments $S_1\to E_1\to I_1$ and $S_2\to E_2\to I_2$, where the latent $(E_1,E_2)$ compartments represent individuals infected but not yet contributing to water contamination, consistent with the biological latency period of the parasite.

### *3.1. Positively invariant region*

In this subsection, we define and analyze the biologically feasible domain for the nondelayed Guinea worm disease model. This region represents the set of all possible states of the system that are meaningful from an epidemiological perspective, ensuring that population sizes remain nonnegative and bounded. We prove that this domain is positively invariant, meaning any trajectory starting within it remains there for all future time. This property is crucial for the model's well-posedness and justifies the subsequent stability analysis conducted within this region.

$$\Sigma=\left\{(S_1,E_1,I_1,S_2,E_2,I_2,I_c)\in\mathbb{R}_+^7:S_1+E_1+I_1\leq\frac{S_1^{in}}{d_1},\ S_2+E_2+I_2\leq\frac{S_2^{in}}{d_2},\ I_c\leq\frac{p_1S_1^{in}}{\varepsilon d_1}+\frac{p_2S_2^{in}}{\varepsilon d_2}\right\}.$$

**Lemma 1.** $\Sigma$ *is a positively invariant, attracting, and compact set for the dynamics of* (3.1).

*Proof.* Since we have $\dot{S}_1 \mid_{S_1=0} = S_1^{in} > 0$, $\dot{E}_1 \mid_{E_1=0} = \beta_1 S_1 I_c > 0$, $\dot{I}_1 \mid_{I_1=0} = \sigma_1 E_1 > 0$, $\dot{S}_2 \mid_{S_2=0} = S_2^{in} > 0$, $\dot{E}_2 \mid_{E_2=0} = \beta_2 S_2 I_c > 0$, $\dot{I}_2 \mid_{I_2=0} = \sigma_2 E_2 > 0$, and $\dot{I}_c \mid_{I_c=0} = p_1 I_1 + p_2 I_2 > 0$. Therefore, $\mathbb{R}^7_+$ is invariant by the dynamics of (3.1). In the context of the Guinea worm disease model, this represents the state space where all compartment populations (susceptible, latent, infectious, and water larvae) take nonnegative values, which is biologically meaningful.

Let us denote by $T_1 := S_1 + E_1 + I_1$ and $T_2 := S_2 + E_2 + I_2$ as the sizes of the total individuals from Patchs 1 and 2, respectively. From the dynamics of (3.1), we have $\dot{T}_1 = S_1^{in} - d_1 S_1 - d_1 E_1 - d_1 I_1 = d_1 \left( \frac{S_1^{in}}{d_1} - T_1 \right)$. Hence, $T_1 = S_1 + E_1 + I_1 \leq \frac{S_1^{in}}{d_1}$ if $T_1(0) = S_1(0) + E_1(0) + I_1(0) \leq \frac{S_1^{in}}{d_1}$.

Similarly, $\dot{T}_2 = S_2 + E_2 + I_2 = S_2^{in} - d_2 S_2 - d_2 E_2 - d_2 I_2 = d_2 \left( \frac{S_2^{in}}{d_2} - T_2 \right)$. Hence, $T_2 = S_2 + E_2 + I_2 \leq \frac{S_2^{in}}{d_2}$ if $T_2(0) = S_2(0) + E_2(0) + I_2(0) \leq \frac{S_2^{in}}{d_2}$. Similarly, $\dot{I}_c = p_1 I_1 + p_2 I_2 - \varepsilon I_c \leq \frac{p_1 S_1^{in}}{d_1} + \frac{p_2 S_2^{in}}{d_2} - \varepsilon I_c$. Hence, $I_c \leq \frac{p_1 S_1^{in}}{\varepsilon d_1} + \frac{p_2 S_2^{in}}{\varepsilon d_2}$ if $I_c(0) \leq \frac{p_1 S_1^{in}}{\varepsilon d_1} + \frac{p_2 S_2^{in}}{\varepsilon d_2}$. Hence, the $\Sigma$ is positively invariant. □

Next, we will derive the basic reproduction number, a fundamental concept in mathematical epidemiology that quantifies the transmission potential of an infectious disease, and then we will analyze the steady states of the dynamics (3.1).

### *3.2. Threshold analysis and steady states*

This subsection is dedicated to the derivation of the basic reproduction number $\mathscr{R}_0$ and the analysis of the system's equilibria. Using the next-generation matrix method [31], we compute $\mathscr{R}_0$, which serves as a critical threshold parameter determining whether the disease persists or dies out. We establish the existence and uniqueness of the disease-free equilibrium and prove that an endemic equilibrium exists if and only if $\mathscr{R}_0 > 1$. This threshold analysis provides the foundational conditions for the global stability results presented in the subsequent subsection. The next-generation matrix is given by $\mathbf{F}\mathbf{V}^{-1}$, where the matrices $\mathbf{F}$ and $\mathbf{V}$ are the fundamental components of the next-generation matrix (NGM) method used to calculate the basic reproduction number, $\mathscr{R}_0$.

The matrices $\mathbf{F}$ and $\mathbf{V}$ are given hereafter:

$$\mathbf{F} = \begin{bmatrix} 0 & 0 & 0 & 0 & \beta_1 \frac{S_1^{in}}{d_1} \\ 0 & 0 & 0 & 0 & \beta_2 \frac{S_2^{in}}{d_2} \\ 0 & 0 & 0 & 0 & 0 \\ 0 & 0 & 0 & 0 & 0 \\ 0 & 0 & 0 & 0 & 0 \end{bmatrix} \text{ and } \mathbf{V} = \begin{bmatrix} \sigma_1 + d_1 & 0 & 0 & 0 & 0 \\ 0 & \sigma_2 + d_2 & 0 & 0 & 0 \\ -\sigma_1 & 0 & d_1 & 0 & 0 \\ 0 & -\sigma_2 & 0 & d_2 & 0 \\ 0 & 0 & -p_1 & -p_2 & \varepsilon \end{bmatrix}.$$

The matrix $\mathbf{F}$ represents the rate at which new infections appear in the infected compartments. In this model, the only entry points for new infections are the latent compartments ($E_1$ and $E_2$) for both host populations. The matrix $\mathbf{V}$ describes all other transitions between and out of the infected compartments. It is defined as $\mathbf{V} = \mathbf{V}^+ - \mathbf{V}^-$, where $\mathbf{V}^-$ is the rate of transfer out of a compartment, and $\mathbf{V}^+$ is the rate of transfer into a compartment from other infected states (but not from new infections). In summary, $\mathbf{F}$

models the birth of new infections, while $\mathbf{V}$ models the "life-history" and death of existing infections within the system. The next-generation matrix is given by $\mathbf{FV}^{-1}$, and its spectral radius, $\rho(\mathbf{FV}^{-1})$, gives the basic reproduction number $\mathscr{R}_0$ as follows:

$$\mathscr{R}_0 = \frac{p_1\beta_1\sigma_1 S_1^{in}}{\varepsilon d_1^2(\sigma_1+d_1)} + \frac{p_2\beta_2\sigma_2 S_2^{in}}{\varepsilon d_2^2(\sigma_2+d_2)} = \mathscr{R}_{01} + \mathscr{R}_{02}. \tag{3.2}$$

We establish the existence and uniqueness of the disease-free equilibrium and prove that an endemic equilibrium exists if and only if $\mathscr{R}_0 > 1$. The following theorem formalizes the existence condition for the endemic equilibrium.

**Theorem 1.** *If $\mathscr{R}_0 > 1$, then* (3.1) *admits a unique endemic steady state.*

*Proof.* Let the endemic steady state of (3.1) be denoted by $\mathscr{E}^* = (S_1^*, S_2^*, E_1^*, E_2^*, I_1^*, I_2^*, I_c^*)$; then it satisfies

$$\begin{cases} 0 &= S_1^{in} - d_1 S_1^* - \beta_1 S_1^* I_c^*, \\ 0 &= \beta_1 S_1^* I_c^* - (d_1+\sigma_1) E_1^*, \\ 0 &= \sigma_1 E_1^* - d_1 I_1^*, \\ 0 &= S_2^{in} - d_2 S_2^* - \beta_2 S_2^* I_c^*, \\ 0 &= \beta_2 S_2 I_c^* - (d_2+\sigma_2) E_2^*, \\ 0 &= \sigma_2 E_2^* - d_2 I_2^*, \\ 0 &= (p_1 I_1^* + p_2 I_2^*) - \varepsilon I_c^*. \end{cases}$$

As $I_c^* \neq 0$, we obtain $S_1^* = \dfrac{S_1^{in}}{d_1+\beta_1 I_c^*}$, $S_2^* = \dfrac{S_2^{in}}{d_2+\beta_2 I_c^*}$, $E_1^* = \dfrac{\beta_1 S_1^{in} I_c^*}{(d_1+\sigma_1)(d_1+\beta_1 I_c^*)}$, $I_1^* = \dfrac{\sigma_1\beta_1 S_1^{in} I_c^*}{d_1(d_1+\sigma_1)(d_1+\beta_1 I_c^*)}$, $E_2^* = \dfrac{\beta_2 S_2^{in} I_c^*}{(d_2+\sigma_2)(d_2+\beta_2 I_c^*)}$, and $I_2^* = \dfrac{\sigma_2\beta_2 S_2^{in} I_c^*}{d_2(d_2+\sigma_2)(d_2+\beta_2 I_c^*)}$, where $I_c^*$ satisfies the following equation:

$$\frac{p_1\sigma_1\beta_1 S_1^{in}}{d_1(d_1+\sigma_1)(d_1+\beta_1 I_c^*)} + \frac{p_2\sigma_2\beta_2 S_2^{in}}{d_2(d_2+\sigma_2)(d_2+\beta_2 I_c^*)} - \varepsilon = 0.$$

Let us consider the function $h$ given by

$$h(I_c) = \frac{p_1\sigma_1\beta_1 S_1^{in}}{d_1(d_1+\sigma_1)(d_1+\beta_1 I_c)} + \frac{p_2\sigma_2\beta_2 S_2^{in}}{d_2(d_2+\sigma_2)(d_2+\beta_2 I_c)} - \varepsilon.$$

Then we have

$$h(0) = \frac{p_1\sigma_1\beta_1 S_1^{in}}{d_1^2(d_1+\sigma_1)} + \frac{p_2\sigma_2\beta_2 S_2^{in}}{d_2^2(d_2+\sigma_2)} - \varepsilon = \varepsilon\left(\frac{p_1\sigma_1\beta_1 S_1^{in}}{\varepsilon d_1^2(d_1+\sigma_1)} + \frac{p_2\sigma_2\beta_2 S_2^{in}}{\varepsilon d_2^2(d_2+\sigma_2)} - 1\right) = \varepsilon(\mathscr{R}_0 - 1).$$

Thus, $h(0) > 0$ when $\mathscr{R}_0 > 1$. Furthermore, we have $h(I_c) \to -\varepsilon < 0$ whenever $I_c \to \infty$. Moreover,

$$h'(I_c) = -\left(\frac{p_1\sigma_1\beta_1^2 S_1^{in}}{d_1(d_1+\sigma_1)(d_1+\beta_1 I_c)^2} + \frac{p_2\sigma_2\beta_2^2 S_2^{in}}{d_2(d_2+\sigma_2)(d_2+\beta_2 I_c)^2}\right) < 0.$$

Thus, $h$ is a strictly decreasing function of $I_c$, and hence, if $\mathscr{R}_0 > 1$, there exists a unique $I_c^* \in (0,\infty)$ such that $h(I_c^*) = 0$. Hence, $S_1^* = \dfrac{S_1^{in}}{d_1+\beta_1 I_c^*} > 0$, $S_2^* = \dfrac{S_2^{in}}{d_2+\beta_2 I_c^*} > 0$, $E_1^* = \dfrac{\beta_1 S_1^{in} I_c^*}{(d_1+\sigma_1)(d_1+\beta_1 I_c^*)} > 0$, $I_1^* =$

$\frac{\sigma_1\beta_1 S_1^{in} I_c^*}{d_1(d_1+\sigma_1)(d_1+\beta_1 I_c^*)} > 0$, $E_2^* = \frac{\beta_2 S_2^{in} I_c^*}{(d_2+\sigma_2)(d_2+\beta_2 I_c^*)} > 0$, and $I_2^* = \frac{\sigma_2\beta_2 S_2^{in} I_c^*}{d_2(d_2+\sigma_2)(d_2+\beta_2 I_c^*)} > 0$. We obtain, for $\mathscr{R}_0 > 1$, a unique endemic equilibrium point given by $\mathscr{E}^* = (S_1^*, E_1^*, I_1^*, S_2^*, E_2^*, I_2^*, I_c^*)$. □

**Remark 1.** *The coupling mechanism through the shared water source $I_c$ deserves special attention. Since both populations rely on the same contaminated water, the concentration of infectious larvae $I_c$ serves as a common driver of infection. If $I_c > 0$, individuals in both patches are exposed, regardless of differences in awareness or behavior. Consequently, the system admits only two types of equilibrium: either $I_c = 0$, in which case both patches are disease-free ($E_1 = E_2 = I_1 = I_2 = 0$), or $I_c > 0$, leading to endemic states in both patches simultaneously. It is impossible for one patch to sustain active transmission while the other remains infection-free, as any positive contribution to $I_c$ from the endemic patch would expose the other patch. This feature is biologically realistic for communities sharing an untreated water source, where contamination places all users at risk.*

In this subsection, we established the fundamental threshold quantity $\mathscr{R}_0$ for the nondelayed model, which dictates the existence and stability of the system's equilibria. We have shown that the disease-free equilibrium is the only steady state when $\mathscr{R}_0 \leq 1$, while a unique endemic equilibrium emerges when $\mathscr{R}_0 > 1$. This clear dichotomy, governed solely by the basic reproduction number, provides the essential theoretical foundation for the subsequent global stability analysis presented in the following subsection.

### *3.3. Global stability analysis of equilibria*

This subsection establishes the global stability properties of the equilibria for the nondelayed Guinea worm disease model. Using carefully constructed Lyapunov functions, we prove that the disease-free equilibrium is globally asymptotically stable when the basic reproduction number satisfies $\mathscr{R}_0 \leq 1$, effectively leading to disease eradication. Conversely, when $\mathscr{R}_0 > 1$, we demonstrate that the unique endemic equilibrium is globally asymptotically stable, indicating persistent disease transmission. These results provide a comprehensive understanding of the long-term behavior of the system under all initial conditions within the biologically feasible region.

**Theorem 2.** *If $\mathscr{R}_0 \leq 1$, then $\mathscr{E}_0$ is globally asymptotically stable (GAS) in $\Sigma$.*

*Proof.* Let us consider the candidate Lyapunov function:

$$\begin{aligned}\mathscr{L}_0 &= \sigma_1\frac{p_1}{d_1}(d_2+\sigma_2)E_1 + \frac{p_1}{d_1}(d_1+\sigma_1)(d_2+\sigma_2)I_1 + \sigma_2\frac{p_2}{d_2}(d_1+\sigma_1)E_2 \\ &\quad + \frac{p_2}{d_2}(d_2+\sigma_2)(d_1+\sigma_1)I_2 + (d_1+\sigma_1)(d_2+\sigma_2)I_c.\end{aligned}$$

By differentiating $\mathscr{L}_0$ along the trajectories of the dynamics of (3.1), we obtain

$$\begin{aligned}\dot{\mathscr{L}}_0 &= \sigma_1\frac{p_1}{d_1}(d_2+\sigma_2)\dot{E}_1 + \frac{p_1}{d_1}(d_1+\sigma_1)(d_2+\sigma_2)\dot{I}_1 + \sigma_2\frac{p_2}{d_2}(d_1+\sigma_1)\dot{E}_2 \\ &\quad + \frac{p_2}{d_2}(d_2+\sigma_2)(d_1+\sigma_1)\dot{I}_2 + (d_1+\sigma_1)(d_2+\sigma_2)\dot{I}_c.\end{aligned}$$

Since $S_1 \leq \frac{S_1^{in}}{d_1}$ and $S_2 \leq \frac{S_2^{in}}{d_2}$ in $\Sigma$, it follows that

$$\begin{aligned}
\dot{\mathscr{L}}_0 &= \varepsilon(d_1+\sigma_1)(d_2+\sigma_2)\left[\frac{\beta_1\sigma_1 p_1 S_1}{\varepsilon d_1(d_1+\sigma_1)}+\frac{\beta_2\sigma_2 p_2 S_2}{\varepsilon d_2(d_2+\sigma_2)}-1\right]I_c \\
&\leq \varepsilon(d_1+\sigma_1)(d_2+\sigma_2)\left[\frac{\beta_1\sigma_1 p_1 S_1^{in}}{\varepsilon d_1^2(d_1+\sigma_1)}+\frac{\beta_2\sigma_2 p_2 S_2^{in}}{\varepsilon d_2^2(d_2+\sigma_2)}-1\right]I_c \\
&= \varepsilon(d_1+\sigma_1)(d_2+\sigma_2)\,(\mathscr{R}_0-1)\,I_c \\
&\leq 0,
\end{aligned}$$

where $\mathscr{R}_0 \leq 1$. When $\mathscr{R}_0 < 1$, $\dot{\mathscr{L}}_0 = 0$ yields $I_c = 0$. Therefore, it can be deduced from system (3.1) that, as $t \to \infty$, $E_1 \to 0$, $E_2 \to 0$, $I_1 \to 0$, $I_2 \to 0$, $S_1 \to \frac{S_1^{in}}{d_1}$, and $S_2 \to \frac{S_2^{in}}{d_2}$. Thus, the invariant set for which $\dot{\mathscr{L}}_0 = 0$ is the singleton $\left\{\mathscr{E}_0 = \left(\frac{S_1^{in}}{d_1}, 0, 0, \frac{S_2^{in}}{d_2}, 0, 0, 0\right)\right\}$. By using Lasalle's invariance principle [32], we deduce that any solution of the dynamics of (3.1) with initial conditions in $\Sigma$ converges to $\mathscr{E}_0$ as $t \to \infty$. Thus, the equilibrium point $\mathscr{E}_0$ is globally asymptotically stable in $\Sigma$ once $\mathscr{R}_0 < 1$. When $\mathscr{R}_0 = 1$, $\dot{\mathscr{L}}_0 = 0$ implies either $I_c = 0$, or

$$1 = \frac{\beta_1\sigma_1 p_1 S_1}{\varepsilon d_1(d_1+\sigma_1)}+\frac{\beta_2\sigma_2 p_2 S_2}{\varepsilon d_2(d_2+\sigma_2)} \leq \frac{\beta_1\sigma_1 p_1 S_1^{in}}{\varepsilon d_1^2(d_1+\sigma_1)}+\frac{\beta_2\sigma_2 p_2 S_2^{in}}{\varepsilon d_2^2(d_2+\sigma_2)} = \mathscr{R}_0.$$

The latter case yields $S_1 = \frac{S_1^{in}}{d_1}$, $S_2 = \frac{S_2^{in}}{d_2}$ and, consequently, $E_1 = I_1 = E_2 = I_2 = I_c = 0$. Therefore, the invariant set for which $\dot{\mathscr{L}}_0 = 0$ is the singleton $\mathscr{E}_0 = \left(\frac{S_1^{in}}{d_1}, 0, 0, \frac{S_2^{in}}{d_2}, 0, 0, 0\right)$. Therefore, the steady state $\mathscr{E}_0$ is globally asymptotically stable in $\Sigma$ if $\mathscr{R}_0 = 1$. □

**Theorem 3.** *If $\mathscr{R}_0 > 1$, the endemic steady state of the dynamics of* (3.1)*, $\mathscr{E}^*$, exists, and is globally asymptotically stable.*

*Proof.* Consider the nonnegative function $\Phi(x) = x - 1 - \ln x$ that only vanishes at $x = 1$, and define a candidate Lyapunov function $\mathscr{F}^*(S_1, E_1, I_1, S_2, E_2, I_2, I_c)$:

$$\begin{aligned}
\mathscr{F}^* &= S_1^*\Phi\left(\frac{S_1}{S_1^*}\right)+E_1^*\Phi\left(\frac{E_1}{E_1^*}\right)+\frac{d_1+\sigma_1}{\sigma_1}I_1^*\Phi\left(\frac{I_1}{I_1^*}\right)+\frac{d_1 p_2\sigma_2(d_1+\sigma_1)}{d_2 p_1\sigma_1(d_2+\sigma_2)}S_2^*\Phi\left(\frac{S_2}{S_2^*}\right) \\
&\quad+\frac{d_1 p_2\sigma_2(d_1+\sigma_1)}{d_2 p_1\sigma_1(d_2+\sigma_2)}E_2^*\Phi\left(\frac{E_2}{E_2^*}\right)+\frac{d_1 p_2(d_1+\sigma_1)}{d_2 p_1\sigma_1}I_2^*\Phi\left(\frac{I_2}{I_2^*}\right)+\frac{d_1(d_1+\sigma_1)}{p_1\sigma_1}I_c^*\Phi\left(\frac{I_c}{I_c^*}\right).
\end{aligned}$$

We calculate $\frac{d\mathscr{F}^*}{dt}$ along the trajectories of dynamics (3.1) to obtain

$$\begin{aligned}
\frac{d\mathscr{F}^*}{dt} &= \left(1-\frac{S_1^*}{S_1}\right)\left(S_1^{in}-d_1S_1-\beta_1S_1I_c\right)+\left(1-\frac{E_1^*}{E_1}\right)\left(\beta_1S_1I_c-(d_1+\sigma_1)E_1\right) \\
&\quad+\frac{d_1+\sigma_1}{\sigma_1}\left(1-\frac{I_1^*}{I_1}\right)\left(\sigma_1E_1-d_1I_1\right)+\frac{d_1p_2\sigma_2(d_1+\sigma_1)}{d_2p_1\sigma_1(d_2+\sigma_2)}\left(1-\frac{S_2^*}{S_2}\right)\left(S_2^{in}-d_2S_2-\beta_2S_2I_c\right) \\
&\quad+\frac{d_1p_2\sigma_2(d_1+\sigma_1)}{d_2p_1\sigma_1(d_2+\sigma_2)}\left(1-\frac{E_2^*}{E_2}\right)\left(\beta_2S_2I_c-(d_2+\sigma_2)E_2\right) \\
&\quad+\frac{d_1p_2(d_1+\sigma_1)}{d_2p_1\sigma_1}\left(1-\frac{I_2^*}{I_2}\right)\left(\sigma_2E_2-d_2I_2\right)+\frac{d_1(d_1+\sigma_1)}{p_1\sigma_1}\left(1-\frac{I_c^*}{I_c}\right)\left(p_1I_1+p_2I_2-mI_c\right).
\end{aligned}$$

By using the equilibrium equalities,

$$S_1^{in} = d_1S_1^* + \beta_1 S_1^* I_c^*,\ S_2^{in} = d_2S_2^* + \beta_2 S_2^* I_c^*,\ (p_1I_1^* + p_2I_2^*) = \varepsilon I_c^*,$$
$$\beta_1 S_1^* I_c^* = (d_1+\sigma_1)E_1^*, \sigma_1 E_1^* = d_1 I_1^*,\ \beta_2 S_2^* I_c^* = (d_2+\sigma_2)E_2^*, \sigma_2 E_2^* = d_2 I_2^*,$$

we get

$$d_1I_1^* = \sigma_1 E_1^* = \frac{\sigma_1\beta_1 S_1^* I_c^*}{(d_1+\sigma_1)}, d_2 I_2^* = \sigma_2 E_2^* = \frac{\sigma_2\beta_2 S_2^* I_c^*}{(d_2+\sigma_2)},$$

and

$$\begin{aligned}
\frac{d\bar{\mathscr{F}}}{dt} &= \left(1-\frac{S_1^*}{S_1}\right)(d_1S_1^* - d_1S_1) + \beta_1 S_1^* I_c^*\left(1-\frac{S_1^*}{S_1}\right) - \beta_1 S_1 I_c \frac{E_1^*}{E_1} + \beta_1 S_1^* I_c^* \\
&\quad -\beta_1 S_1^* I_c^* \frac{I_1^*}{I_1}\frac{E_1}{E_1^*} + \beta_1 S_1^* I_c^* + \frac{d_1p_2\sigma_2(d_1+\sigma_1)}{d_2p_1\sigma_1(d_2+\sigma_2)}\left(1-\frac{S_2^*}{S_2}\right)(d_2S_2^* - d_2S_2) \\
&\quad +\frac{d_1p_2\sigma_2(d_1+\sigma_1)}{d_2p_1\sigma_1(d_2+\sigma_2)}\beta_2 S_2^* I_c^*\left(1-\frac{S_2^*}{S_2}\right) - \frac{d_1p_2\sigma_2(d_1+\sigma_1)}{d_2p_1\sigma_1(d_2+\sigma_2)}\beta_2 S_2^* I_c^* \frac{S_2 I_c E_2^*}{S_2^* I_c^* E_2} \\
&\quad +\frac{d_1p_2\sigma_2(d_1+\sigma_1)}{d_2p_1\sigma_1(d_2+\sigma_2)}\beta_2 S_2^* I_c^* - \frac{d_1p_2\sigma_2(d_1+\sigma_1)}{d_2p_1\sigma_1(d_2+\sigma_2)}\beta_2 S_2^* I_c^* \frac{I_2^*}{I_2}\frac{E_2}{E_2^*} \\
&\quad +\frac{d_1p_2\sigma_2(d_1+\sigma_1)}{d_2p_1\sigma_1(d_2+\sigma_2)}\beta_2 S_2^* I_c^* - \beta_1 S_1^* I_c^* \frac{I_1}{I_1^*}\frac{I_c^*}{I_c} - \frac{d_1p_2\sigma_2(d_1+\sigma_1)}{d_2p_1\sigma_1(d_2+\sigma_2)}\beta_2 S_2^* I_c^* \frac{I_2}{I_2^*}\frac{I_c^*}{I_c} \\
&\quad +\beta_1 S_1^* I_c^* + \frac{d_1p_2\sigma_2(d_1+\sigma_1)}{d_2p_1\sigma_1(d_2+\sigma_2)}\beta_2 S_2^* I_c^*.
\end{aligned}$$

Therefore,

$$\begin{aligned}
\frac{d\mathscr{F}^*}{dt} &= -\frac{d_1(S_1-S_1^*)^2}{S_1} - \frac{d_1p_2\sigma_2(d_1+\sigma_1)}{d_2p_1\sigma_1(d_2+\sigma_2)}\frac{d_2(S_2-S_2^*)^2}{S_2} \\
&\quad +\beta_1 S_1^* I_c^*\left(4 - \frac{S_1^*}{S_1} - \frac{I_1 I_c^*}{I_1^* I_c} - \frac{I_1^* E_1}{I_1 E_1^*} - \frac{S_1 I_c E_1^*}{S_1^* I_c^* E_1}\right) \\
&\quad +\frac{d_1p_2\sigma_2(d_1+\sigma_1)}{d_2p_1\sigma_1(d_2+\sigma_2)}\beta_2 S_2^* I_c^*\left(4 - \frac{S_2^*}{S_2} - \frac{I_2 I_c^*}{I_2^* I_c} - \frac{I_2^* E_2}{I_2 E_2^*} - \frac{S_2 I_c E_2^*}{S_2^* I_c^* E_2}\right).
\end{aligned}$$

Hence $\frac{d\mathscr{F}^*}{dt} \leq 0$. Moreover, $\frac{d\mathscr{F}^*}{dt} = 0$ if $(S_1, E_1, I_1, S_2, E_2, I_2, I_c) = (S_1^*, E_1^*, I_1^*, S_2^*, E_2^*, I_2^*, I_c^*)$. LaSalle's invariance principle indicates that $\mathscr{E}^*$ is GAS when $\mathscr{R}_0 > 1$. □

In conclusion, the global stability analysis conducted in this subsection rigorously demonstrates the decisive role of the basic reproduction number $\mathscr{R}_0$ in determining the long-term dynamics of the Guinea worm disease model. The construction of suitable Lyapunov functions has proven that the disease-free equilibrium is globally asymptotically stable when $\mathscr{R}_0 \leq 1$, ensuring the eventual eradication of the disease from the population. Conversely, when $\mathscr{R}_0 > 1$, the unique endemic equilibrium is globally asymptotically stable, indicating that the disease will persist regardless of the initial number of infections. These powerful results confirm the threshold behavior of the system and underscore the critical importance of reducing $\mathscr{R}_0$ below unity for effective disease control.

## 4. Dynamics of the delayed model and the influence of time lags

Building upon the analysis of the nondelayed system, this section extends the model by incorporating discrete delays to more accurately represent the biological time lags inherent in the Guinea worm disease transmission cycle. These delays account for critical processes such as the latent period within human hosts and the development time of the parasite in the water environment. We investigate the impact of these temporal factors on the system's dynamics, beginning with the definition of a biologically feasible domain for the delayed system. Subsequently, we derive the delayed basic reproduction number $\mathscr{R}_0^d$ and analyze the existence and stability of equilibria. The section culminates in a comprehensive global stability analysis, paralleling the results of the nondelayed case but now expressed in terms of the modified threshold $\mathscr{R}_0^d$, thereby quantifying how time delays influence the potential for disease eradication or persistence.

### *4.1. Biological feasibility*

Before analyzing the dynamical behavior of the delayed system, it is essential to establish the domain in which the model variables remain biologically meaningful. Since the state variables represent population counts and pathogen concentrations, they must remain nonnegative and bounded for all time. The following lemma demonstrates that the nonnegative orthant is positively invariant under the flow of the delayed system and that all trajectories eventually enter a compact region, ensuring that the model is well-posed from both biological and mathematical perspectives. This invariant region serves as the natural setting for the subsequent stability analysis.

Let us define the survival probabilities $F_i = e^{-m_i \iota_i}$ for $i = 1, \cdots, 5$. By considering the following set

$$\begin{aligned}\Sigma^d \quad = \Bigg\{ & (S_1, E_1, I_1, S_2, E_2, I_2, I_c) \in \mathbb{R}_+^7 : \|S_1\| \leq \frac{S_1^{in}}{d_1}, \|E_1\| \leq \frac{S_1^{in}}{d_1}, \|I_1\| \leq \frac{\sigma_1 S_1^{in}}{d_1^2}, \\ & \|S_2\| \leq \frac{S_2^{in}}{d_2}, \|E_2\| \leq \frac{S_2^{in}}{d_2}, \|I_2\| \leq \frac{\sigma_2 S_2^{in}}{d_2^2}, \|I_c\| \leq \frac{p_1 \sigma_1 S_1^{in}}{d_1^2 \varepsilon} + \frac{p_2 \sigma_2 S_2^{in}}{d_2^2 \varepsilon} \Bigg\},\end{aligned}$$

we obtain the following lemma.

**Lemma 2** (Nonnegativity and ultimate boundedness)**.** *Trajectories of system (2.1) with the initial values (2) are nonnegative for all $t \geq 0$. Moreover, all trajectories are ultimately bounded; in particular, there exists a finite time $T > 0$ such that for all $t > T$, the trajectory remains within the bounded region $\Sigma^d$. The nonnegative orthant $\mathbb{R}_+^7$ is positively invariant under the flow of the system (2.1).*

*Proof.* Clearly, $\dot{S}_1 \mid_{S_1=0} = S_1^{in} > 0$, $\dot{S}_2 \mid_{S_2=0} = S_2^{in} > 0$. Hence, $S_1(t) > 0$ and $S_2(t) > 0$ for any $t \geq 0$. In addition, we have

$$\begin{aligned}E_1(t) &= e^{-(d_1+\sigma_1)t}\phi_1^E(0) + \beta_1 F_1 \int_0^t e^{-(d_1+\sigma_1)(t-\theta)} S_1(\theta - \iota_1) I_c(\theta - \iota_1) d\theta \geq 0, \\ I_1(t) &= e^{-d_1 t}\phi_1^I(0) + \sigma_1 F_2 \int_0^t e^{-d_1(t-\theta)} E_1(\theta - \iota_2) d\theta \geq 0, \\ E_2(t) &= e^{-(d_2+\sigma_2)t}\phi_2^E(0) + \beta_2 F_3 \int_0^t e^{-(d_2+\sigma_2)(t-\theta)} S_2(\theta - \iota_3) I_c(\theta - \iota_3) d\theta \geq 0,\end{aligned}$$

$$I_2(t) = e^{-d_2 t}\phi_2^I(0) + \sigma_2 F_4 \int_0^t e^{-d_2(t-\theta)} E_2(\theta - \iota_4) d\theta \geq 0,$$
$$I_c(t) = e^{-\varepsilon t}\phi^V(0) + F_5 \int_0^t e^{-\varepsilon(t-\theta)} [p_1 I_1(\theta - \iota_5) + p_2 I_2(\theta - \iota_5)] d\theta \geq 0,$$

for any $t \in [0, \iota^*]$. Therefore, by recursive argumentation, we deduce that

$$(S_1, E_1, I_1, S_2, E_2, I_2, I_c)(t) \geq 0 \text{ for any } t \geq 0.$$

According to the first equation of dynamics (2.1), we get $\limsup_{t\to\infty} S_1(t) \leq \frac{S_1^{in}}{d_1}$. Let us define

$$\psi_1(t) = S_1(t) + \frac{1}{F_1} E_1(t + \iota_1).$$

Then, we get

$$\begin{aligned}
\dot{\psi}_1(t) &= \dot{S}_1(t) + \frac{1}{F_1}\dot{E}_1(t+\iota_1) \\
&= S_1^{in} - d_1 S_1(t) - \beta_1 S_1(t) I_c(t) + \beta_1 S_1(t) I_c(t) - (d_1 + \sigma_1)\frac{1}{F_1} E_1(t+\iota_1) \\
&\leq d_1 \left( \frac{S_1^{in}}{d_1} - S_1(t) - \frac{1}{F_1} E_1(t+\iota_1) \right) \\
&= d_1 \left( \frac{S_1^{in}}{d_1} - \psi_1(t) \right).
\end{aligned}$$

It follows that $\limsup_{t\to\infty} \psi_1(t) \leq \frac{S_1^{in}}{d_1}$, and then $\limsup_{t\to\infty} E_1(t) \leq \frac{S_1^{in}}{d_1}$. Similarly, we have

$$\dot{I}_1(t) = \sigma_1 F_2 E_1(t - \iota_2) - d_1 I_1(t) \leq \sigma_1 F_2 \frac{S_1^{in}}{d_1} - d_1 I_1(t) \leq \sigma_1 \frac{S_1^{in}}{d_1} - d_1 I_1(t).$$

It follows that $\limsup_{t\to\infty} I_1(t) \leq \frac{\sigma_1 S_1^{in}}{d_1^2}$. Similarly, let us define

$$\psi_2(t) = S_2(t) + \frac{1}{F_3} E_2(t + \iota_3).$$

Then, we get

$$\begin{aligned}
\dot{\psi}_2(t) &= \dot{S}_2(t) + \frac{1}{F_3}\dot{E}_2(t+\iota_3) \\
&= S_2^{in} - d_2 S_2(t) - \beta_2 S_2(t) I_c(t) + \beta_2 S_2(t) I_c(t) - \frac{1}{F_3}(d_2 + \sigma_2) E_2(t+\iota_3) \\
&\leq d_2 \left( \frac{S_2^{in}}{d_2} - S_2(t) - \frac{1}{F_3} E_2(t+\iota_3) \right) \\
&= d_2 \left( \frac{S_2^{in}}{d_2} - \psi_2(t) \right).
\end{aligned}$$

It follows that $\limsup_{t\to\infty} \psi_2(t) \leq \frac{S_2^{in}}{d_2}$, and then $\limsup_{t\to\infty} E_2(t) \leq \frac{S_2^{in}}{d_2}$. Note that

$$\dot{I}_2(t) = \sigma_2 F_4 E_2(t-\iota_4) - d_2 I_2(t) \leq \sigma_2 F_4 \frac{S_2^{in}}{d_2} - d_2 I_2(t) \leq \sigma_2 \frac{S_2^{in}}{d_2} - d_2 I_2(t).$$

It follows that $\limsup_{t\to\infty} I_2(t) \leq \frac{\sigma_2 S_2^{in}}{d_2^2}$. In the same way, we get

$$\dot{I}_c(t) = F_5[p_1 I_1(t-\iota_5) + p_2 I_2(t-\iota_5)] - \varepsilon I_c(t) \leq \frac{p_1\sigma_1 S_1^{in}}{d_1^2} + \frac{p_2\sigma_2 S_2^{in}}{d_2^2} - \varepsilon I_c(t).$$

It follows that $\limsup_{t\to\infty} I_c(t) \leq \frac{p_1\sigma_1 S_1^{in}}{d_1^2\varepsilon} + \frac{p_2\sigma_2 S_2^{in}}{d_2^2\varepsilon}$. Therefore, one deduces that $\Sigma^d$ is a positively invariant with respect to system (2.1). □

Lemma 2 confirms that the delayed Guinea worm disease model is mathematically well-posed and epidemiologically consistent. By demonstrating that all state variables remain nonnegative and ultimately bounded for all time, we have provided a rigorous foundation for the subsequent analysis of equilibrium stability and threshold dynamics (see [33, 34] for similar applications).

### *4.2. Threshold analysis and equilibrium states of the delayed system*

This subsection focuses on deriving the fundamental threshold quantity for the delayed Guinea worm disease model and analyzing the existence of its equilibrium points. We employ the next-generation matrix method [31] to compute the delayed basic reproduction number $\mathscr{R}_0^d$, which incorporates the effects of discrete time lags through exponential delay factors. The matrices $\mathbf{F}_d$ and $\mathbf{V}_d$, representing new infections and transitions between compartments, respectively, are constructed to account for these temporal delays. We then establish the existence and uniqueness conditions for both the disease-free equilibrium $\mathscr{E}_0^d$ and the endemic equilibrium $\mathscr{E}_d^*$, demonstrating that the threshold $\mathscr{R}_0^d = 1$ continues to serve as the critical boundary between disease eradication and persistence, even in the presence of explicit time delays in the transmission dynamics.

The matrices $\mathbf{F}_d$ and $\mathbf{V}_d$ used in this construction are given as follows:

$$\mathbf{F}_d = \begin{pmatrix} 0 & 0 & 0 & 0 & F_1\beta_1\frac{S_1^{in}}{d_1} \\ 0 & 0 & 0 & 0 & 0 \\ 0 & 0 & 0 & 0 & F_3\beta_2\frac{S_2^{in}}{d_2} \\ 0 & 0 & 0 & 0 & 0 \\ 0 & 0 & 0 & 0 & 0 \end{pmatrix}, \mathbf{V}_d = \begin{pmatrix} d_1+\sigma_1 & 0 & 0 & 0 & 0 \\ -\sigma_1 F_2 & d_1 & 0 & 0 & 0 \\ 0 & 0 & d_2+\sigma_2 & 0 & 0 \\ 0 & 0 & -\sigma_2 F_4 & d_2 & 0 \\ 0 & -p_1 F_5 & 0 & -p_2 F_5 & \varepsilon \end{pmatrix}.$$

Therefore,

$$\mathscr{R}_0^d = \rho(\mathbf{F}_d \mathbf{V}_d^{-1}) = \mathscr{R}_{01}^d + \mathscr{R}_{02}^d,$$

where

$$\mathscr{R}_{01}^d = \frac{p_1\sigma_1\beta_1 S_1^{in}}{\varepsilon d_1^2(d_1+\sigma_1)} F_1F_2F_5 \text{ and } \mathscr{R}_{02}^d = \frac{p_2\sigma_2\beta_2 S_2^{in}}{\varepsilon d_2^2(d_2+\sigma_2)} F_3F_4F_5.$$

We establish the existence and uniqueness of the disease-free equilibrium and prove that an endemic equilibrium exists if and only if $\mathscr{R}_0^d > 1$. The following theorem formalizes the existence condition for the endemic equilibrium.

**Theorem 4.** • *The system (2.1) admits an infection-free equilibrium denoted by*

$$\mathscr{E}_0^d = \left(\frac{S_1^{in}}{d_1}, 0, 0, \frac{S_2^{in}}{d_2}, 0, 0, 0\right).$$

• *If $\mathscr{R}_0^d > 1$, then the system (2.1) admits an endemic equilibrium point denoted by*

$$\mathscr{E}_d^* = (S_1^*, E_1^*, I_1^*, S_2^*, E_2^*, I_2^*, I_c^*).$$

*Proof.* The steady-states satisfy

$$\begin{cases} 0 &= S_1^{in} - d_1 S_1 - \beta_1 S_1 I_c, \\ 0 &= \beta_1 F_1 S_1 I_c - (d_1 + \sigma_1) E_1, \\ 0 &= \sigma_1 F_2 E_1 - d_1 I_1, \\ 0 &= S_2^{in} - d_2 S_2 - \beta_2 S_2 I_c, \\ 0 &= \beta_2 F_3 S_2 I_c - (d_2 + \sigma_2) E_2, \\ 0 &= \sigma_2 F_4 E_2 - d_2 I_2, \\ 0 &= F_5(p_1 I_1 + p_2 I_2) - \varepsilon I_c. \end{cases}$$

We have the following two cases:

1. If $I_c = 0$, the system admits an infection-free equilibrium point $\mathscr{E}_0^d = \left(\frac{S_1^{in}}{d_1}, 0, 0, \frac{S_2^{in}}{d_2}, 0, 0, 0\right)$.

2. If $I_c \neq 0$, we obtain

$$S_1 = \frac{S_1^{in}}{d_1 + \beta_1 I_c},\ S_2 = \frac{S_2^{in}}{d_2 + \beta_2 I_c},\ E_1 = \frac{\beta_1 F_1 S_1^{in} I_c}{(d_1 + \sigma_1)(d_1 + \beta_1 I_c)},$$
$$I_1 = \frac{\sigma_1 \beta_1 F_1 F_2 S_1^{in} I_c}{d_1 (d_1 + \sigma_1)(d_1 + \beta_1 I_c)}, E_2 = \frac{\beta_2 F_3 S_2^{in} I_c}{(d_2 + \sigma_2)(d_2 + \beta_2 I_c)}, I_2 = \frac{\sigma_2 \beta_2 F_3 F_4 S_2^{in} I_c}{d_2 (d_2 + \sigma_2)(d_2 + \beta_2 I_c)},$$

and $I_c$ satisfies the following equation:

$$\frac{p_1 \sigma_1 \beta_1 F_1 F_2 F_5 S_1^{in}}{d_1 (d_1 + \sigma_1)(d_1 + \beta_1 I_c)} + \frac{p_2 \sigma_2 \beta_2 F_3 F_4 F_5 S_2^{in}}{d_2 (d_2 + \sigma_2)(d_2 + \beta_2 I_c)} - \varepsilon = 0.$$

Let us consider the function $h$ given by

$$h(I_c) = \frac{p_1 \sigma_1 \beta_1 F_1 F_2 F_5 S_1^{in}}{d_1 (d_1 + \sigma_1)(d_1 + \beta_1 I_c)} + \frac{p_2 \sigma_2 \beta_2 F_3 F_4 F_5 S_2^{in}}{d_2 (d_2 + \sigma_2)(d_2 + \beta_2 I_c)} - \varepsilon.$$

Then, we have

$$\begin{aligned} h(0) &= \frac{p_1 \sigma_1 \beta_1 F_1 F_2 F_5 S_1^{in}}{d_1^2 (d_1 + \sigma_1)} + \frac{p_2 \sigma_2 \beta_2 F_3 F_4 F_5 S_2^{in}}{d_2^2 (d_2 + \sigma_2)} - \varepsilon \\ &= \varepsilon \left( \frac{p_1 \sigma_1 \beta_1 F_1 F_2 F_5 S_1^{in}}{\varepsilon d_1^2 (d_1 + \sigma_1)} + \frac{p_2 \sigma_2 \beta_2 F_3 F_4 F_5 S_2^{in}}{\varepsilon d_2^2 (d_2 + \sigma_2)} - 1 \right) \\ &= \varepsilon \left( \mathscr{R}_0^d - 1 \right). \end{aligned}$$

Thus, $h(0) > 0$ when $\mathscr{R}_0^d > 1$. Furthermore, we have $h(I_c) \to -\varepsilon < 0$ whenever $I_c \to \infty$. Moreover,

$$h'(I_c) = -\left( \frac{p_1\sigma_1\beta_1^2 F_1F_2F_5S_1^{in}}{d_1(d_1+\sigma_1)(d_1+\beta_1 I_c)^2} + \frac{p_2\sigma_2\beta_2^2 F_3F_4F_5S_2^{in}}{d_2(d_2+\sigma_2)(d_2+\beta_2 I_c)^2} \right) < 0.$$

Thus, $h$ is a strictly decreasing function of $I_c$, and hence, if $\mathscr{R}_0^d > 1$, there exists a unique $I_c^* \in (0,\infty)$ such that $h(I_c^*) = 0$. Hence, $S_1^* = \dfrac{S_1^{in}}{d_1+\beta_1 I_c^*} > 0$, $S_2^* = \dfrac{S_2^{in}}{d_2+\beta_2 I_c^*} > 0$, $E_1^* = \dfrac{\beta_1 F_1 S_1^{in} I_c^*}{(d_1+\sigma_1)(d_1+\beta_1 I_c^*)} > 0$, $I_1^* = \dfrac{\sigma_1\beta_1 F_1F_2 S_1^{in} I_c^*}{d_1(d_1+\sigma_1)(d_1+\beta_1 I_c^*)} > 0$, $E_2^* = \dfrac{\beta_2 F_3 S_2^{in} I_c^*}{(d_2+\sigma_2)(d_2+\beta_2 I_c^*)} > 0$, and $I_2^* = \dfrac{\sigma_2\beta_2 F_3F_4 S_2^{in} I_c^*}{d_2(d_2+\sigma_2)(d_2+\beta_2 I_c^*)} > 0$. We obtain, for $\mathscr{R}_0^d > 1$, a unique endemic equilibrium point given by $\mathscr{E}_d^* = (S_1^*, E_1^*, I_1^*, S_2^*, E_2^*, I_2^*, I_c^*)$.

□

**Remark 2.** *The delays do not alter the structure of the endemic equilibrium but quantitatively reduce the equilibrium population sizes of infected compartments through the factors $F_i = e^{-m_i \iota_i}$.*

In conclusion, this subsection has extended the threshold analysis to the delayed Guinea worm disease model (2.1), deriving the delayed basic reproduction number $\mathscr{R}_0^d$ and characterizing the system's equilibria. The expression for $\mathscr{R}_0^d = \mathscr{R}_{01}^d + \mathscr{R}_{02}^d$ explicitly incorporates the discrete delays through exponential terms, quantitatively demonstrating that time lags in the parasite's life cycle reduce the overall transmission potential. We have rigorously established that the disease-free equilibrium $\mathscr{E}_0^d$ is the only steady state when $\mathscr{R}_0^d \leq 1$, while a unique endemic equilibrium $\mathscr{E}_d^*$ exists if and only if $\mathscr{R}_0^d > 1$. This threshold condition, which mirrors the structure of the nondelayed case while accounting for temporal delays, provides the critical foundation for the global stability results presented in the subsequent subsection.

### *4.3. Global stability analysis for the delayed system*

This subsection establishes the global stability properties of the equilibria for the delayed Guinea worm disease model, extending the results from the nondelayed case to the more biologically realistic scenario incorporating time lags. Through the construction of sophisticated Lyapunov functionals that explicitly account for the discrete delays, we prove that the disease-free equilibrium $\mathscr{E}_0^d$ is globally asymptotically stable when $\mathscr{R}_0^d \leq 1$. Furthermore, when $\mathscr{R}_0^d > 1$, we demonstrate that the unique endemic equilibrium $\mathscr{E}_d^*$ is globally asymptotically stable. These results confirm that the threshold dynamics observed in the nondelayed system persist in the delayed model, with the delayed basic reproduction number $\mathscr{R}_0^d$ serving as the crucial parameter governing the long-term behavior of the system, regardless of initial conditions within the biologically feasible region.

**Theorem 5.** *The infection-free equilibrium point $\mathscr{E}_0^d$ is GAS once $\mathscr{R}_0^d \leq 1$.*

*Proof.* Let us consider a candidate Lyapunov function $\mathscr{F}_0^d(S_1,E_1,I_1,S_2,E_2,I_2,I_c)$ given by

$$\begin{aligned}\mathscr{F}_0^d &= F_1F_2F_5\frac{S_1^{in}}{d_1}\Phi\left(\frac{d_1S_1}{S_1^{in}}\right)+F_2F_5E_1+F_5\frac{d_1+\sigma_1}{\sigma_1}I_1+F_3F_4F_5\frac{d_1p_2\sigma_2(d_1+\sigma_1)}{d_2p_1\sigma_1(d_2+\sigma_2)}\frac{S_2^{in}}{d_2}\Phi\left(\frac{d_2S_2}{S_2^{in}}\right)\\
&+F_4F_5\frac{d_1p_2\sigma_2(d_1+\sigma_1)}{d_2p_1\sigma_1(d_2+\sigma_2)}E_2+F_5\frac{d_1p_2(d_1+\sigma_1)}{d_2p_1\sigma_1}I_2+\frac{d_1(d_1+\sigma_1)}{p_1\sigma_1}I_c+F_1F_2F_5\beta_1\int_{t-\iota_1}^{t}S_1(\theta)I_c(\theta)d\theta\\
&+F_2F_5(d_1+\sigma_1)\int_{t-\iota_2}^{t}E_1(\theta)d\theta+F_3F_4F_5\beta_2\frac{d_1p_2\sigma_2(d_1+\sigma_1)}{d_2p_1\sigma_1(d_2+\sigma_2)}\int_{t-\iota_3}^{t}S_2(\theta)I_c(\theta)d\theta\\
&+F_4F_5\frac{d_1p_2\sigma_2(d_1+\sigma_1)}{d_2p_1\sigma_1}\int_{t-\iota_4}^{t}E_2(\theta)d\theta+\frac{d_1(d_1+\sigma_1)}{p_1\sigma_1}F_5\int_{t-\iota_5}^{t}\big(p_1I_1(\theta)+p_2I_2(\theta)\big)d\theta.\end{aligned}$$

By applying the LaSalle's invariance principle, we deduce that $\mathscr{E}_0$ is GAS if $\mathscr{R}_0^d\leq 1$. More details are given in appendix A.1. □

**Theorem 6.** *If the dual target-infection equilibrium point $\mathscr{E}_d^*$ exists ($\mathscr{R}_0^d>1$), then it is GAS.*

*Proof.* The proof is based on the Lyapunov function $\mathscr{F}_d^*(S_1,E_1,I_1,S_2,E_2,I_2,I_c)$ given by

$$\begin{aligned}\mathscr{F}_d^* &= F_1F_2F_5S_1^*\Phi\left(\frac{S_1}{S_1^*}\right)+F_2F_5E_1^*\Phi\left(\frac{E_1}{E_1^*}\right)+F_5\frac{d_1+\sigma_1}{\sigma_1}I_1^*\Phi\left(\frac{I_1}{I_1^*}\right)\\
&+F_3F_4F_5\frac{d_1p_2\sigma_2(d_1+\sigma_1)}{d_2p_1\sigma_1(d_2+\sigma_2)}S_2^*\Phi\left(\frac{S_2}{S_2^*}\right)+F_4F_5\frac{d_1p_2\sigma_2(d_1+\sigma_1)}{d_2p_1\sigma_1(d_2+\sigma_2)}E_2^*\Phi\left(\frac{E_2}{E_2^*}\right)\\
&+F_5\frac{d_1p_2(d_1+\sigma_1)}{d_2p_1\sigma_1}I_2^*\Phi\left(\frac{I_2}{I_2^*}\right)+\frac{d_1(d_1+\sigma_1)}{p_1\sigma_1}I_c^*\Phi\left(\frac{I_c}{I_c^*}\right)\\
&+F_1F_2F_5\beta_1S_1^*I_c^*\int_{t-\iota_1}^{t}\Phi\left(\frac{S_1(\theta)I_c(\theta)}{S_1^*I_c^*}\right)d\theta+F_2F_5(d_1+\sigma_1)E_1^*\int_{t-\iota_2}^{t}\Phi\left(\frac{E_1(\theta)}{E_1^*}\right)d\theta\\
&+F_3F_4F_5\beta_2\frac{d_1p_2\sigma_2(d_1+\sigma_1)}{d_2p_1\sigma_1(d_2+\sigma_2)}S_2^*I_c^*\int_{t-\iota_3}^{t}\Phi\left(\frac{S_2(\theta)I_c(\theta)}{S_2^*I_c^*}\right)d\theta\\
&+F_4F_5\frac{d_1p_2\sigma_2(d_1+\sigma_1)}{d_2p_1\sigma_1}E_2^*\int_{t-\iota_4}^{t}\Phi\left(\frac{E_2(\theta)}{E_2^*}\right)d\theta\\
&+F_5\frac{d_1(d_1+\sigma_1)}{p_1\sigma_1}\int_{t-\iota_5}^{t}\left(p_1I_1^*\Phi\left(\frac{I_1(\theta)}{I_1^*}\right)+p_2I_2^*\Phi\left(\frac{I_2(\theta)}{I_2^*}\right)\right)d\theta,\end{aligned}$$

and by using LaSalle's invariance principle to prove that $\mathscr{E}_d^*$ is GAS if $\mathscr{R}_0^d>1$. More details are given in appendix A.2. □

In conclusion, the global stability analysis for the delayed system has been rigorously established through the construction of appropriate Lyapunov functionals that explicitly incorporate the discrete delays. We have proven that the disease-free equilibrium $\mathscr{E}_0^d$ is globally asymptotically stable when $\mathscr{R}_0^d\leq 1$, ensuring disease eradication, while the endemic equilibrium $\mathscr{E}_d^*$ is globally asymptotically stable when $\mathscr{R}_0^d>1$, indicating persistent disease transmission. These results demonstrate that the fundamental threshold dynamics characterized by the basic reproduction number are preserved in the delayed system, with $\mathscr{R}_0^d$ serving as the critical parameter governing long-term behavior. The analytical findings confirm that the incorporation of biologically relevant time delays does not alter the qualitative behavior of the system but quantitatively modifies the stability conditions through the exponential delay terms in $\mathscr{R}_0^d$.

## 5. Simulation analysis of Guinea worm disease dynamics

In this section, we present a comprehensive numerical simulation analysis aimed at exploring the dynamics of Guinea worm disease (GWD) through the mathematical model developed in earlier sections. Utilizing MATLAB's dde23 solver, we investigate the stability of equilibria and the effects of treatment interventions, time delays, and parameter sensitivity on disease transmission. This analysis not only serves to validate the theoretical predictions derived from the model but also provides valuable insights into optimal control strategies for effective disease management in varying scenarios. Through numerical experimentation, we aim to illustrate the practical implications of our findings and to evaluate the robustness of our model under different conditions.

### *5.1. Equilibrium stability assessment*

In this subsection, we focus on the assessment of stability for the equilibria of the Guinea worm disease model. By employing numerical simulations, we aim to determine the conditions under which the disease-free and endemic equilibria are stable or unstable. This analysis is essential for understanding the long-term behavior of the disease dynamics and for evaluating the effectiveness of various control strategies. We will explore how changes in key parameters influence the stability criteria, thereby providing crucial insights for designing interventions aimed at eradicating Guinea worm disease. Our approach utilizes the mathematical framework established in previous sections to analyze the stability characteristics of the model through simulation outcomes. For all numerical simulations, we suppose that constants $m_i = 1$ and the delays $\iota_i = 0.1$ for $i = 1, \cdots, 5$. Some parameters are fixed and given in Table 2 hereafter. Since there are no real data for Guinea worm disease, we state that the used parameters, including those given in Table 2, are chosen arbitrarily to satisfy the threshold conditions ($\mathscr{R}_0^d < 1$ or $> 1$) for illustrative purposes.

**Table 2.** Parameter values.

| Parameter | $S_1^{in}$ | $S_2^{in}$ | $\sigma_1$ | $\sigma_2$ | $d_1$ | $d_2$ | $p_1$ | $p_2$ | $\varepsilon$ |
|---|---|---|---|---|---|---|---|---|---|
| Value | 20 | 10 | 0.01 | 0.03 | 0.02 | 0.01 | 0.01 | 0.003 | 0.4 |

We consider four main cases using the parameter values given in Table 2 as follows:

- For $\beta_1 = 0.0003$ and $\beta_2 = 0.0006$, we get a basic reproduction number $\mathscr{R}_0 = 0.46 < 1$, predicting disease eradication according to Theorem 2.
- For $\beta_1 = 0.003$ and $\beta_2 = 0.004$, we get a basic reproduction number $\mathscr{R}_0 = 3.5 > 1$, predicting the persistence of the disease according to Theorem 3.
- For $\beta_1 = 0.0003$ and $\beta_2 = 0.0006$, we get a basic reproduction number $\mathscr{R}_0^d = 0.34 < 1$, predicting disease eradication according to Theorem 5.
- For $\beta_1 = 0.003$ and $\beta_2 = 0.004$, we get a basic reproduction number $\mathscr{R}_0^d = 2.59 > 1$, predicting the persistence of the disease according to Theorem 6.

Figure 2 illustrates the dynamics of Guinea worm disease in the absence of delays when the basic reproduction number satisfies $\mathscr{R}_0 = 0.46 < 1$. Under this condition, both susceptible and infected populations in the two host patches decline over time, signaling disease eradication. The

lack of sustained transmission confirms the model's theoretical prediction that eradication is feasible with appropriate interventions. This scenario underscores the critical importance of maintaining low infection rates and implementing preventive measures to interrupt the transmission cycle.

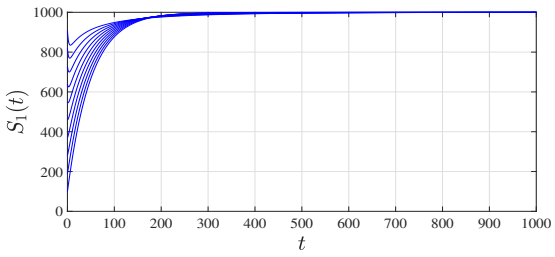


**(a)** Uninfected individuals (Batch 1).

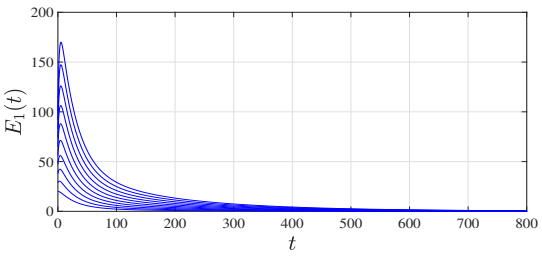


**(b)** Latent infected individuals (Batch 1).

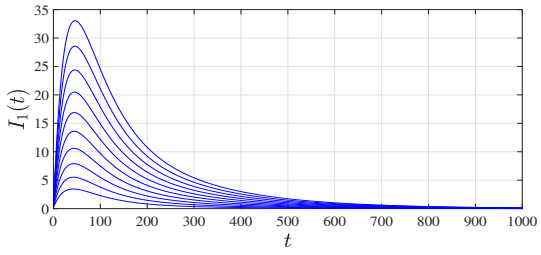


**(c)** Active infected individuals (Batch 1).

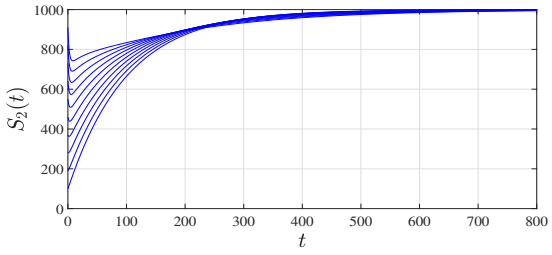


**(d)** Uninfected individuals (Batch 2).

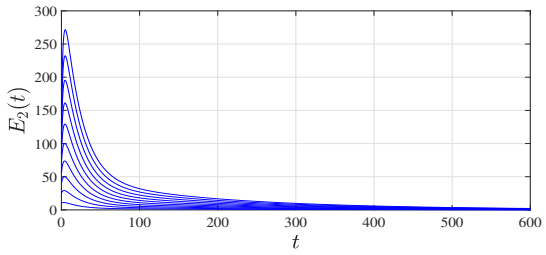


**(e)** Latent infected individuals (Batch 2).

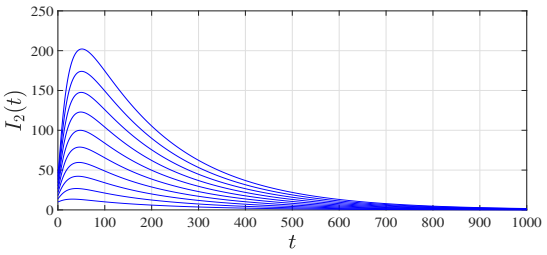


**(f)** Active infected individuals (Batch 2).

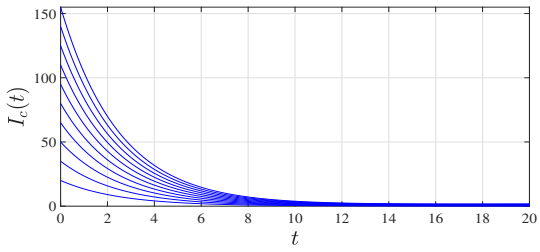


**(g)** Infected copepods in the environment.

**Figure 2.** Dynamics of Guinea worm disease without delays in the absence of treatment with $\mathscr{R}_0 = 0.46 < 1$ for several initial conditions.

Figure 3 depicts the dynamics of Guinea worm disease in the absence of delays when the basic reproduction number exceeds unity $\mathscr{R}_0 = 3.5 > 1$. In this regime, the populations of both latent and actively infectious individuals increase over time, indicating ongoing transmission and the potential for

disease outbreaks. The distinct dynamical patterns observed between the two host populations reflect differences in their susceptibility and immune response to the infection. This finding underscores the urgent need for interventions aimed at reducing transmission rates, as uncontrolled disease dynamics are predicted to result in persistent infection and pose substantial public health challenges.

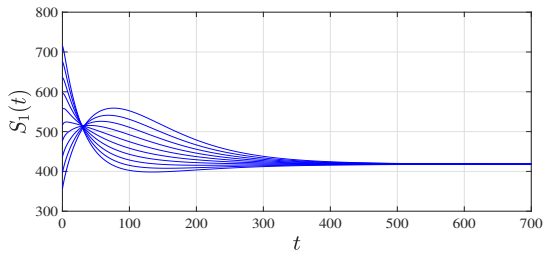


**(a)** Uninfected individuals (Batch 1).

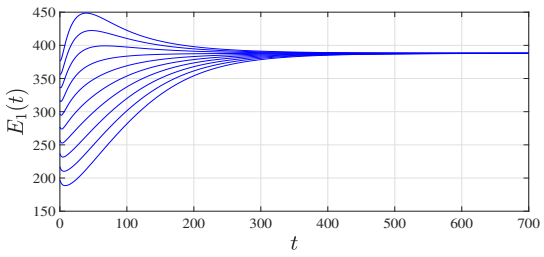


**(b)** Latent infected individuals (Batch 1).

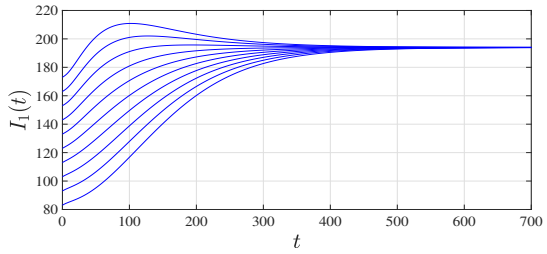


**(c)** Active infected individuals (Batch 1).

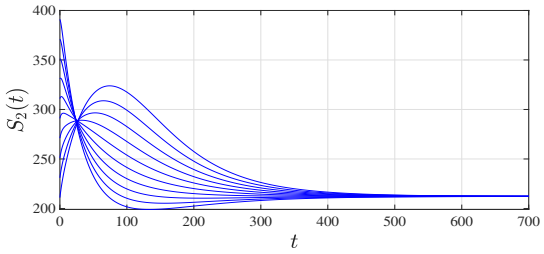


**(d)** Uninfected individuals (Batch 2).

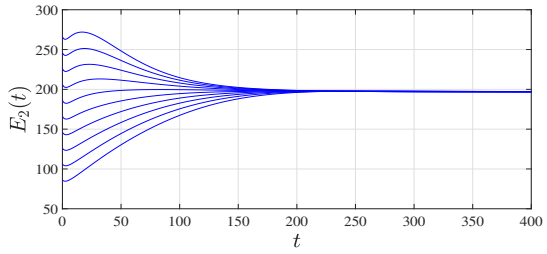


**(e)** Latent infected individuals (Batch 2).

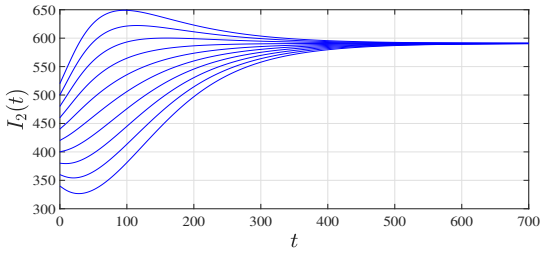


**(f)** Active infected individuals (Batch 2).

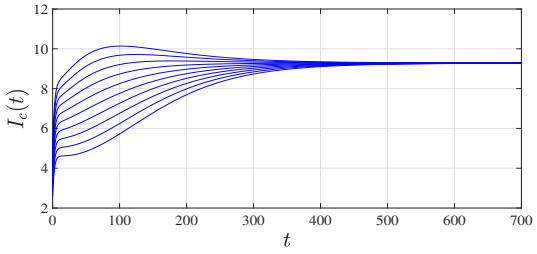


**(g)** Infected copepods in the environment.

**Figure 3.** Dynamics of Guinea worm disease without delays with increased transmission rates and $\mathscr{R}_0 = 3.5 > 1$ for several initial conditions.

In Figure 4, we observe the dynamics of Guinea worm disease under conditions where the basic reproduction number $\mathscr{R}_0^d = 0.34 < 1$. The populations of uninfected and infected individuals in

both host populations demonstrate a decline over time, indicating disease eradication. The absence of sustained transmission corroborates the model's prediction that disease eradication is achievable through appropriate interventions. This scenario highlights the importance of maintaining low infection rates and implementing preventive measures to block the transmission cycle.

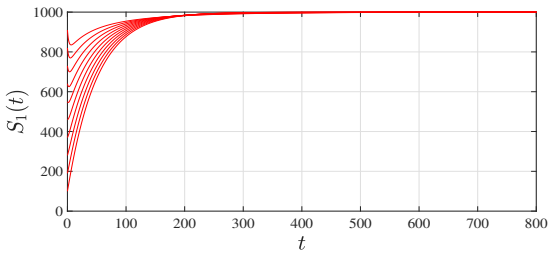


**(a)** Uninfected individuals (Batch 1).

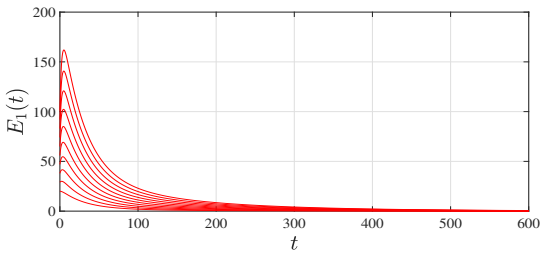


**(b)** Latent infected individuals (Batch 1).

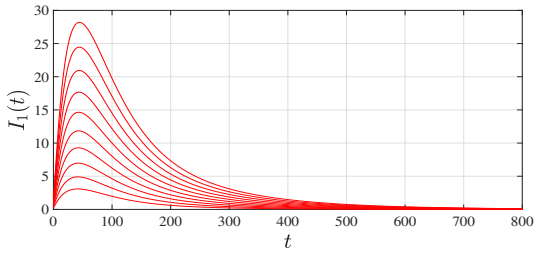


**(c)** Active infected individuals (Batch 1).

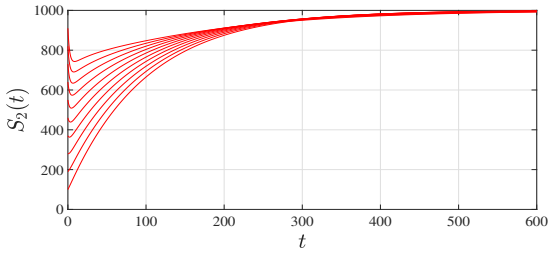


**(d)** Uninfected individuals (Batch 2).

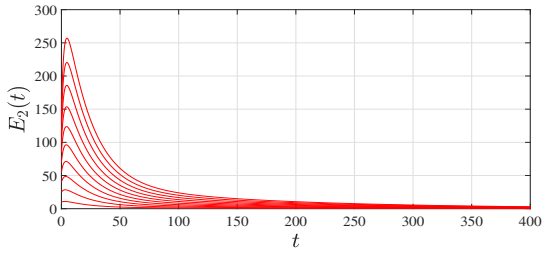


**(e)** Latent infected individuals (Batch 2).

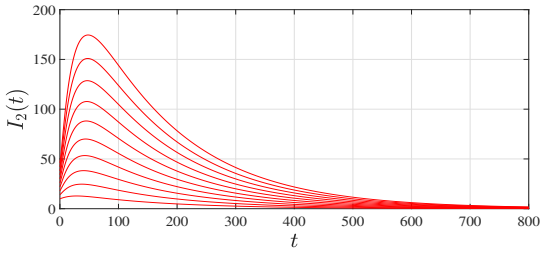


**(f)** Active infected individuals (Batch 2).

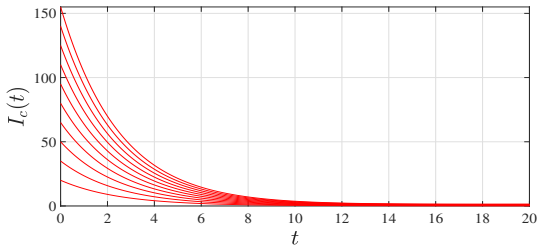


**(g)** Infected copepods in the environment.

**Figure 4.** Dynamics of Guinea worm disease in the absence of treatment with $\mathscr{R}_0^d = 0.34 < 1$ for several initial values.

Figure 5 illustrates the dynamics of Guinea worm disease when the basic reproduction number $\mathscr{R}_0^d = 2.59 > 1$. In this scenario, we witness an increase in the populations of latent and

actively infected individuals, suggesting ongoing transmission and potential disease outbreaks. The clear distinction between the dynamics of both host populations indicates differing susceptibility and response to the disease. This figure emphasizes the critical need for interventions to reduce transmission rates, as the model predicts that unchecked disease dynamics may lead to persistent infection and significant public health challenges.

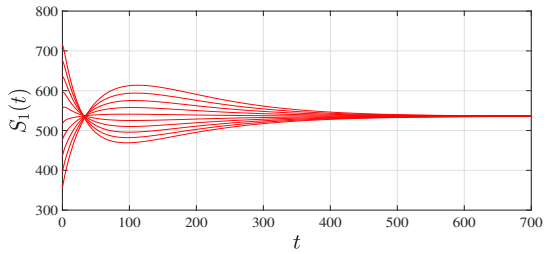


**(a)** Uninfected individuals (Batch 1).

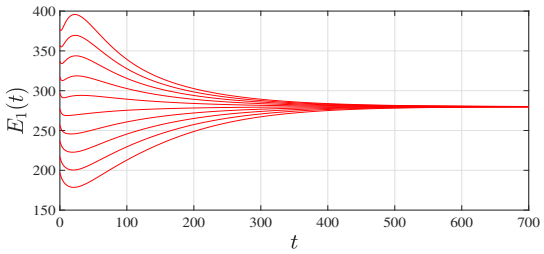


**(b)** Latent infected individuals (Batch 1).

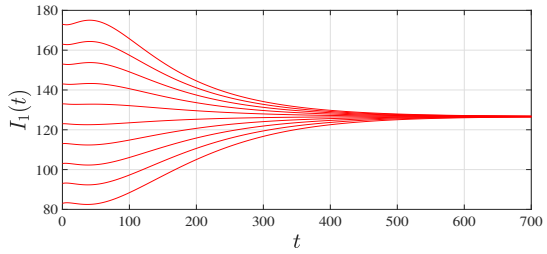


**(c)** Active infected individuals (Batch 1).

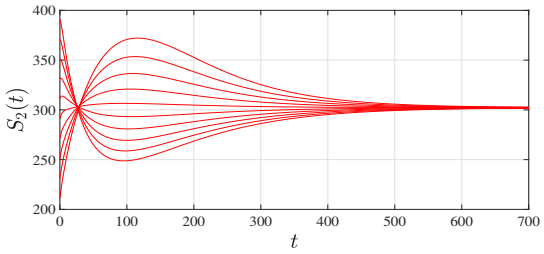


**(d)** Uninfected individuals (Batch 2).

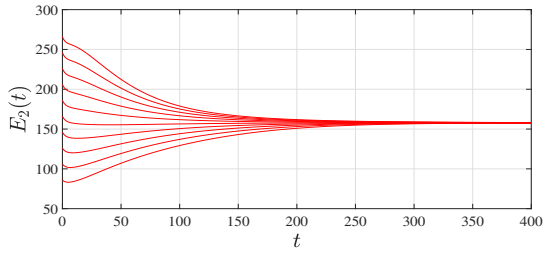


**(e)** Latent infected individuals (Batch 2).

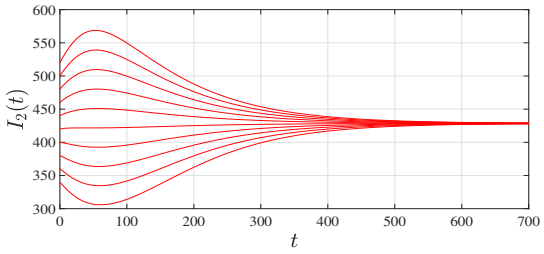


**(f)** Active infected individuals (Batch 2).

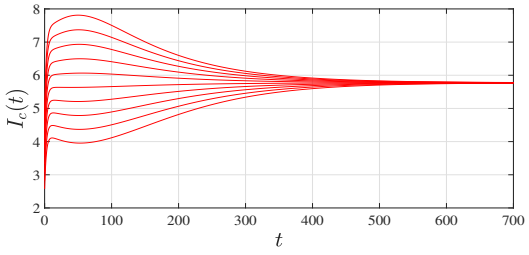


**(g)** Infected copepods in the environment.

**Figure 5.** Dynamics of Guinea worm disease with increased transmission rates and $\mathscr{R}_0^d = 2.59 > 1$ for several initial values.

*5.2. Influence of key parameters on model outputs: A sensitivity perspective*

In this subsection, we investigate how variations in the model parameters affect the basic reproduction number and the overall transmission dynamics of Guinea worm disease. Sensitivity analysis [35] provides a quantitative framework for identifying which biological or epidemiological factors exert the strongest influence on disease spread, thereby revealing leverage points for effective intervention. By computing normalized sensitivity indices, we systematically assess the relative contribution of each parameter to the magnitude of the delayed basic reproduction number, $\mathscr{R}_0^d$, and highlight those parameters whose alteration—through treatment, behavioral change, or environmental management—can produce the most substantial reductions in disease transmission. This analysis not only enhances our understanding of model robustness but also guides the prioritization of public health strategies in heterogeneous settings.

To quantify the influence of each parameter on the delayed basic reproduction number $\mathscr{R}_0^d$, we employ the normalized forward sensitivity index. For a differentiable quantity $\mathscr{R}_0^d = \mathscr{R}_0^d(\theta)$ depending on a parameter $\theta$, its (normalized) sensitivity index is defined by $\Upsilon_\theta^{\mathscr{R}_0^d} = \dfrac{\partial \mathscr{R}_0^d}{\partial \theta} \times \dfrac{\theta}{\mathscr{R}_0^d}$. This dimensionless index measures the relative change in $U$ resulting from a relative change in $\theta$, thereby indicating whether $U$ is increasing or decreasing with respect to that parameter and quantifying the strength of this dependence. In the context of this study, we compute $\Upsilon_\theta^{\mathscr{R}_0^d}$ for all biological and epidemiological parameters $\theta$ appearing in the expression of the delayed reproduction number. In our case, the basic reproduction number $\mathscr{R}_0^d$ is given by

$$\mathscr{R}_0^d = \frac{\sigma_1 p_1 \beta_1 S_1^{in}}{\varepsilon d_1^2 (d_1+\sigma_1)} e^{-(m_1\iota_1+m_2\iota_2+m_5\iota_5)} + \frac{\sigma_2 p_2 \beta_2 S_2^{in}}{\varepsilon d_2^2 (d_2+\sigma_2)} e^{-(m_3\iota_3+m_4\iota_4+m_5\iota_5)}.$$

Therefore, we can easily obtain the sensitivity indices as follows:

$$\begin{aligned}
&\Upsilon_{S_1^{in}}^{\mathscr{R}_0^d} = \Upsilon_{p_1}^{\mathscr{R}_0^d} = \Upsilon_{\beta_1}^{\mathscr{R}_0^d} = \frac{\sigma_1 p_1 \beta_1 S_1^{in}}{\varepsilon d_1^2 \mathscr{R}_0^d (d_1+\sigma_1)} e^{-(m_1\iota_1+m_2\iota_2+m_5\iota_5)},\\
&\Upsilon_{S_2^{in}}^{\mathscr{R}_0^d} = \Upsilon_{p_2}^{\mathscr{R}_0^d} = \Upsilon_{\beta_2}^{\mathscr{R}_0^d} = \frac{\sigma_2 p_2 \beta_2 S_2^{in}}{\varepsilon d_2^2 \mathscr{R}_0 (d_2+\sigma_2)} e^{-(m_3\iota_3+m_4\iota_4+m_5\iota_5)},\\
&\Upsilon_{\sigma_1}^{\mathscr{R}_0^d} = \frac{\sigma_1 p_1 \beta_1 S_1^{in}}{\mathscr{R}_0^d \varepsilon d_1 (d_1+\sigma_1)^2} e^{-(m_1\iota_1+m_2\iota_2+m_5\iota_5)}, \Upsilon_{\sigma_2}^{\mathscr{R}_0^d} = \frac{\sigma_2 p_2 \beta_2 S_2^{in}}{\mathscr{R}_0 \varepsilon d_2 (d_2+\sigma_2)^2} e^{-(m_3\iota_3+m_4\iota_4+m_5\iota_5)},\\
&\Upsilon_{m_1}^{\mathscr{R}_0^d} = \Upsilon_{\iota_1}^{\mathscr{R}_0^d} = -\frac{m_1\iota_1\sigma_1 p_1 \beta_1 S_1^{in}}{\varepsilon d_1^2 (d_1+\sigma_1)\mathscr{R}_0} e^{-(m_1\iota_1+m_2\iota_2+m_5\iota_5)}, \Upsilon_{m_2}^{\mathscr{R}_0} = \Upsilon_{\iota_2}^{\mathscr{R}_0^d} = -\frac{m_2\iota_2\sigma_1 p_1 \beta_1 S_1^{in}}{\varepsilon d_1^2 (d_1+\sigma_1)\mathscr{R}_0^d} e^{-(m_1\iota_1+m_2\iota_2+m_5\iota_5)},\\
&\Upsilon_{m_3}^{\mathscr{R}_0^d} = \Upsilon_{\iota_3}^{\mathscr{R}_0^d} = -\frac{m_3\iota_3\sigma_2 p_2 \beta_2 S_2^{in}}{\varepsilon d_2^2 (d_2+\sigma_2)\mathscr{R}_0} e^{-(m_3\iota_3+m_4\iota_4+m_5\iota_5)}, \Upsilon_{m_4}^{\mathscr{R}_0^d} = \Upsilon_{\iota_4}^{\mathscr{R}_0^d} = -\frac{m_4\iota_4\sigma_2 p_2 \beta_2 S_2^{in}}{\varepsilon d_2^2 (d_2+\sigma_2)\mathscr{R}_0^d} e^{-(m_3\iota_3+m_4\iota_4+m_5\iota_5)},\\
&\Upsilon_{d_1}^{\mathscr{R}_0^d} = -\frac{\sigma_1 p_1 \beta_1 S_1^{in}}{\varepsilon d_1 (d_1+\sigma_1)\mathscr{R}_0^d}\left(\frac{2}{d_1}+\frac{1}{d_1+\sigma_1}\right) e^{-(m_1\iota_1+m_2\iota_2+m_5\iota_5)},\\
&\Upsilon_{d_2}^{\mathscr{R}_0^d} = -\frac{\sigma_2 p_2 \beta_2 S_2^{in}}{\varepsilon d_2 (d_2+\sigma_2)\mathscr{R}_0^d}\left(\frac{2}{d_2}+\frac{1}{d_2+\sigma_2}\right) e^{-(m_3\iota_3+m_4\iota_4+m_5\iota_5)}, \Upsilon_{m_5}^{\mathscr{R}_0^d} = \Upsilon_{\iota_5}^{\mathscr{R}_0^d} = -m_5\iota_5, \Upsilon_{\varepsilon}^{\mathscr{R}_0^d} = -1.
\end{aligned}$$

For $\beta_1 = 0.0003$, $\beta_2 = 0.0006$, and the parameters values given in Table 2, we get the numerical values of the sensitivity indices in Table 3. Positive (negative) values indicate that increasing the parameter increases (decreases) $\mathscr{R}_0^d$.

**Table 3.** Sensitivity indices of the delayed basic reproduction number $\mathscr{R}_0^d$ with respect to model parameters.

| Parameter $\theta$ | $\Upsilon_\theta^{\mathscr{R}_0^d}$ |
|---|---|
| $S_1^{in}, p_1, \beta_1$ | 0.357 |
| $S_2^{in}, p_2, \beta_2$ | 0.643 |
| $\sigma_1$ | 0.238 |
| $\sigma_2$ | 0.161 |
| $\iota_1, m_1, \iota_2, m_2$ | $-0.036$ |
| $\iota_3, m_3, \iota_4, m_4$ | $-0.06$ |
| $m_5, \iota_5$ | $-0.1$ |
| $d_1$ | $-0.238$ |
| $d_2$ | $-0.161$ |
| $\varepsilon$ | $-1$ |

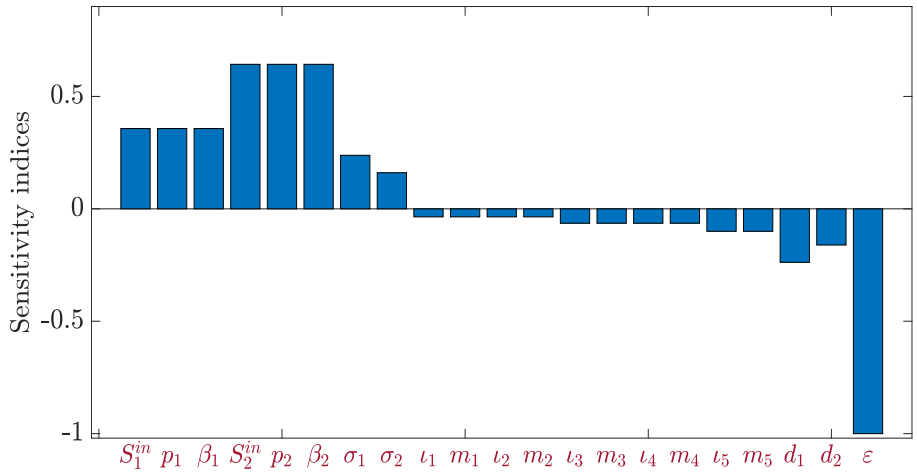


**Figure 6.** Bar chart of sensitivity indices for parameters influencing the delayed basic reproduction number $\mathscr{R}_0^d$. Parameters are ordered by the magnitude of their impact on disease transmission.

Table 3 and Figure 6 present the results of a sensitivity analysis of the delayed basic reproduction number $\mathscr{R}_0^d$ for the Guinea worm disease model. The sensitivity indices quantify how changes in each parameter influence $\mathscr{R}_0^d$, which determines whether the disease will persist or die out.

Parameters with positive sensitivity indices, such as the recruitment rates $S_1^{in}$ and $S_2^{in}$, infection rates $\beta_1$ and $\beta_2$, shedding rates $p_1$ and $p_2$, and progression rates $\sigma_1$ and $\sigma_2$, increase the delayed basic reproduction number $\mathscr{R}_0^d$ when they are increased. Higher recruitment or infection rates lead to more disease transmission, while increased shedding or progression rates also elevate $\mathscr{R}_0^d$. Conversely, parameters with negative sensitivity indices, including the natural death rates $d_1$ and $d_2$, the pathogen decay rate $\varepsilon$, the delays $\iota_i$, and the delay decay rates $m_i$, decrease $\mathscr{R}_0^d$ when increased. Higher natural death rates reduce the number of infectious individuals, an increased pathogen decay rate shortens the lifespan of infectious larvae in the water, and longer delays or higher delay decay rates reduce the

probability of survival through latent or infectious stages, thereby lowering $\mathscr{R}_0^d$. Among all parameters, the most influential are the pathogen decay rate $\varepsilon$ with an index of $-1$, the Patch 2 parameters $S_2^{in}$, $p_2$, and $\beta_2$, each with an index of 0.6429, and the Patch 1 parameters $d_1$ and $\sigma_1$, with indices of $-0.2381$ and 0.2381, respectively. This analysis highlights that interventions targeting the reduction of infection rates $(\beta_1, \beta_2)$, shedding rates $(p_1, p_2)$, or increasing the pathogen decay rate $(\varepsilon)$ would be most effective in controlling Guinea worm disease.

### *5.3. Impact of treatment interventions on disease control*

This subsection investigates the role of treatment interventions in controlling Guinea worm disease dynamics within the two-patch delayed model. We introduce a treatment efficacy parameter $\kappa \in [0,1]$ that reduces the effective infection rates in both patches, representing interventions such as health education, water filtration, and case containment. The modified basic reproduction number $\mathscr{R}_0^{\text{treatment}}(\kappa) = (1-\kappa)\mathscr{R}_0^d$ reveals a direct relationship between treatment efficacy and transmission potential. We derive a critical treatment threshold $\kappa^{\text{cr}} = 1 - 1/\mathscr{R}_0^d$ that determines whether the disease can be eradicated. Through numerical simulations, we analyze how varying levels of treatment efficacy influence disease dynamics and identify the minimum intervention effort required to achieve disease elimination in endemic settings.

By adding a treatment efficacy parameter $\kappa \in [0,1]$, the mathematical model takes the following form:

$$\begin{cases} \dot{S}_1 &= S_1^{in} - d_1 S_1 - (1-\kappa)\beta_1 S_1 I_c, \\ \dot{E}_1 &= (1-\kappa)\beta_1 e^{-m_1 \iota_1} S_1(t-\iota_1) I_c(t-\iota_1) - (d_1+\sigma_1)E_1, \\ \dot{I}_1 &= \sigma_1 e^{-m_2 \iota_2} E_1(t-\iota_2) - d_1 I_1, \\ \dot{S}_2 &= S_2^{in} - d_2 S_2 - (1-\kappa)\beta_2 S_2 I_c, \\ \dot{E}_2 &= (1-\kappa)\beta_2 e^{-m_3 \iota_3} S_2(t-\iota_3) I_c(t-\iota_3) - (d_2+\sigma_2)E_2, \\ \dot{I}_2 &= \sigma_2 e^{-m_4 \iota_4} E_2(t-\iota_4) - d_2 I_2, \\ \dot{V}_c &= e^{-m_5 \iota_5}\left[p_1 I_1(t-\iota_5) + p_2 I_2(t-\iota_5)\right] - \varepsilon I_c. \end{cases} \tag{5.1}$$

According to the reproductive number $\mathscr{R}_0^d$ discussed previously, the basic reproductive number for model (5.1) is given by $\mathscr{R}_0^{\text{treatment}}(\kappa) = (1-\kappa)\mathscr{R}_0^d \leq \mathscr{R}_0^d$. Suppose that $\mathscr{R}_0^d > 1$, and that our objective is to impose $\mathscr{R}_0^{\text{treatment}}(\kappa) \leq 1$ and then the stability of the infection-free equilibrium point $\mathscr{E}_0^d$. The critical treatment efficacy $\kappa^{\text{cr}}$ is given by

$$\mathscr{R}_0^{\text{treatment}}(\kappa^{\text{cr}}) \quad = 1 \Longrightarrow \kappa^{\text{cr}} = 1 - \frac{1}{\mathscr{R}_0^d}.$$

Then, we get $\mathscr{R}_0^{\text{treatment}}(\kappa) \leq 1$ for all $\kappa^{\text{cr}} \leq \kappa \leq 1$, and thus $\mathscr{E}_0$ is GAS. By choosing $\beta_1 = 0.003$ and $\beta_2 = 0.004$, we get $\kappa^{\text{cr}} \approx 0.61$. Therefore,

**(i)** if $0.61 \leq \kappa \leq 1$, then $\mathscr{R}_0^{\text{treatment}}(\kappa) \leq 1$, and $\mathscr{E}_0^d$ is GAS;
**(ii)** if $0 \leq \kappa < 0.61$, then $\mathscr{R}_0^{\text{treatment}}(\kappa) > 1$, and $\mathscr{E}_0^d$ becomes unstable while $\mathscr{E}_d^*$ becomes GAS.

Values below the critical threshold $\kappa^{\text{cr}}$ maintain disease persistence, while higher values lead to eradication.

**Table 4.** Relationship between treatment efficacy $\kappa$ and $\mathscr{R}_0^{\text{treatment}}(\kappa)$.

| $\kappa$ | 0.4 | 0.5 | 0.61 | 0.7 | 0.8 |
|---|---|---|---|---|---|
| $\mathscr{R}_0^{\text{treatment}}(\kappa)$ | 1.56 | 1.3 | 1 | 0.78 | 0.52 |

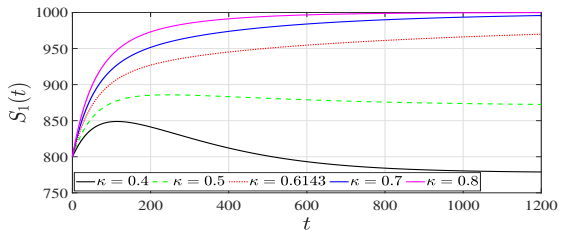


**(a)** Uninfected individuals (Batch 1).

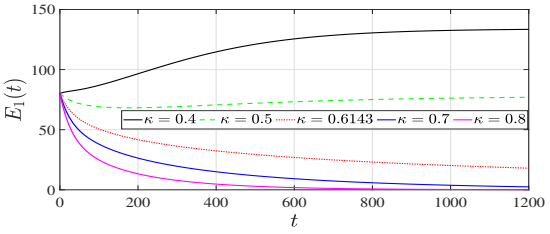


**(b)** Latent infected individuals (Batch 1).

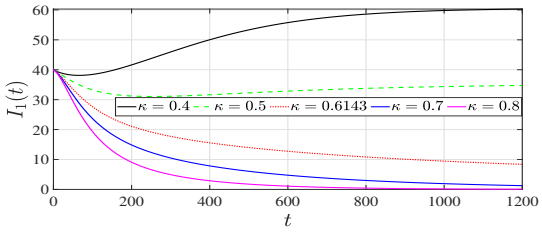


**(c)** Active infected individuals (Batch 1).

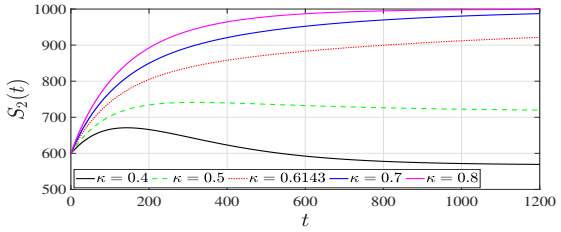


**(d)** Uninfected individuals (Batch 2).

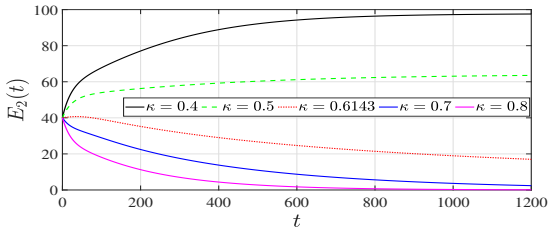


**(e)** Latent infected individuals (Batch 2).

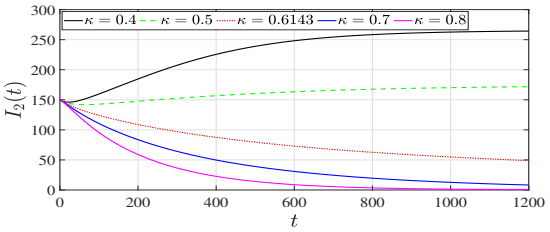


**(f)** Active infected individuals (Batch 2).

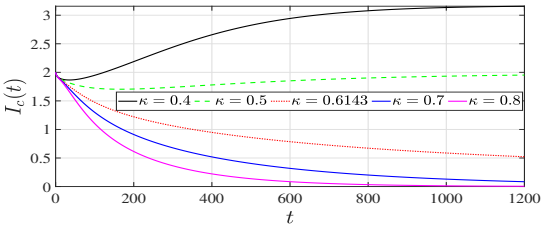


**(g)** Infected copepods in the environment.

**Figure 7.** Disease dynamics under varying treatment efficacy levels $\kappa$. Higher treatment effectiveness accelerates the decline of infected populations, with complete eradication achieved when $\kappa \geq 0.6143$ for the initial values $(800, 80, 40, 600, 40, 150, 2)$.

Table 4 and Figure 7 demonstrate the critical relationship between treatment efficacy and Guinea worm disease dynamics. The treatment efficacy parameter $\kappa$ represents the effectiveness of interventions such as health education, water filtration, and case containment in reducing

disease transmission.

- Table 4 shows that as treatment efficacy $\kappa$ increases from 0.4 to 0.8, the basic reproduction number $\mathscr{R}_0^{\text{treatment}}(\kappa)$ decreases monotonically from 1.56 to 0.52.
- The critical threshold occurs at $\kappa^{\text{cr}} = 0.61$, where $\mathscr{R}_0^{\text{treatment}}(\kappa) = 1$. This represents the minimum treatment efficacy required to achieve disease eradication.
- For $\kappa < \kappa^{\text{cr}}$ (e.g., $\kappa = 0.4, 0.5$), the disease persists as $\mathscr{R}_0^{\text{treatment}}(\kappa) > 1$, leading to endemic equilibrium.
- For $\kappa \geq \kappa^{\text{cr}}$ (e.g., $\kappa = 0.61, 0.7, 0.8$), the disease-free equilibrium becomes globally stable, ensuring eventual disease eradication.
- Figure 7 visually confirms these theoretical predictions, showing how higher treatment efficacy leads to faster decline in infected compartments across both patches, with complete disease elimination achieved when $\kappa \geq 0.61$.

These results highlight that achieving at least 61% effectiveness in control measures is essential for successful Guinea worm eradication, providing a quantitative target for public health interventions.

### *5.4. Effect of time delays on transmission dynamics*

This subsection examines how temporal delays in the Guinea worm life cycle influence disease transmission and control prospects. The analysis focuses particularly on the environmental delay $\iota_5$, which represents the time required for larvae to develop into infectious forms within copepods in the water source. We derive a critical delay threshold $\iota_5^{cr} \approx 1.0528$ that serves as a bifurcation point between disease persistence and eradication. Through numerical simulations, we demonstrate that longer developmental delays in the aquatic environment naturally suppress disease transmission by reducing the basic reproduction number $\mathscr{R}_0^d(\iota_5)$. This investigation provides important insights into how biological time scales interact with intervention strategies, revealing that environmental factors affecting parasite development can significantly enhance or compromise control efforts.

$\iota_5$ appears explicitly in the analytical expression of $\mathscr{R}_0^d$, and any modification of this delay directly influences the stability properties of $\mathscr{E}_0^d$.

Recall that $\mathscr{R}_0^d(\iota_5) = e^{-m_5\iota_5}\left(\dfrac{\sigma_1 p_1\beta_1 S_1^{in}}{\varepsilon d_1^2(d_1+\sigma_1)}e^{-m_1\iota_1-m_2\iota_2} + \dfrac{\sigma_2 p_2\beta_2 S_2^{in}}{\varepsilon d_2^2(d_2+\sigma_2)}e^{-m_3\iota_3-m_4\iota_4}\right)$. Therefore, to impose that $\mathscr{R}_0^d(\iota_5) \leq 1$, we calculate the critical threshold of $\iota_5$ as follows:

$$\iota_5^{cr} = \max\left\{0, \frac{1}{m_5}\ln\left(\frac{\sigma_1 p_1\beta_1 S_1^{in}}{\varepsilon d_1^2(d_1+\sigma_1)}e^{-m_1\iota_1-m_2\iota_2} + \frac{\sigma_2 p_2\beta_2 S_2^{in}}{\varepsilon d_2^2(d_2+\sigma_2)}e^{-m_3\iota_3-m_4\iota_4}\right)\right\},$$

which is approximated by $\iota_5^{cr} \simeq 1.05$ for $\beta_1 = 0.003$ and $\beta_2 = 0.004$. It follows that

- if $\iota_5^{cr} \geq 1.05$, then $\mathscr{R}_0^d(\iota_5) \leq 1$, ensuring the global stability of the infection-free equilibrium point $\mathscr{E}_0^d$.
- However, if $\iota_5^{cr} < 1.05$, $\mathscr{R}_0^d(\iota_5) > 1$, and in this case the endemic equilibrium point becomes globally attractive.

Delays exceeding the critical threshold $\iota_5^{cr} \approx 1.05$ lead to disease eradication through increased larval mortality.

**Table 5.** Influence of environmental development delay $\iota_5$ on $\mathscr{R}_0^d(\iota_5)$.

| $\iota_5$ | 0.2 | 0.5 | 1.05 | 1.5 | 2 |
|---|---|---|---|---|---|
| $\mathscr{R}_0^d(\iota_5)$ | 2.35 | 1.74 | 1 | 0.64 | 0.3878 |

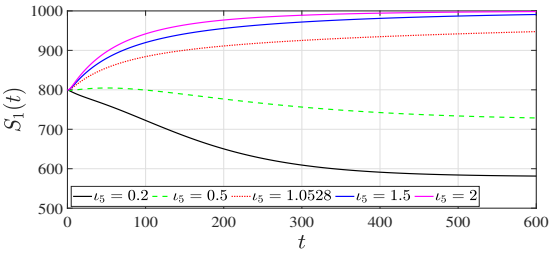


**(a)** Uninfected individuals (Batch 1).

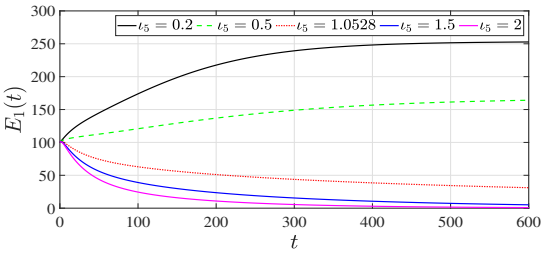


**(b)** Latent infected individuals (Batch 1).

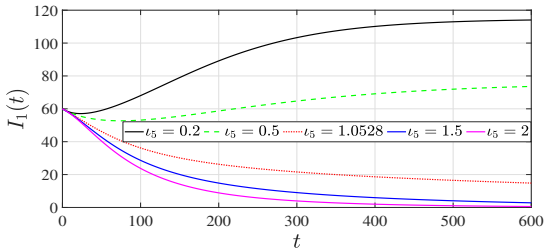


**(c)** Active infected individuals (Batch 1).

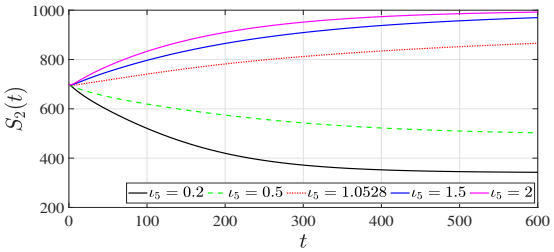


**(d)** Uninfected individuals (Batch 2).

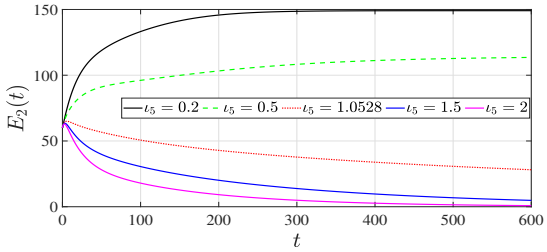


**(e)** Latent infected individuals (Batch 2).

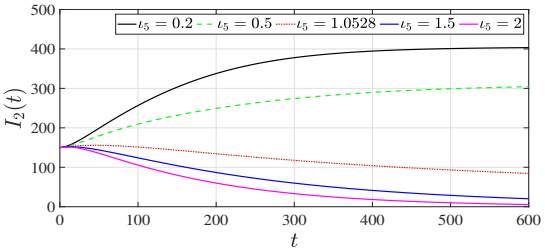


**(f)** Active infected individuals (Batch 2).

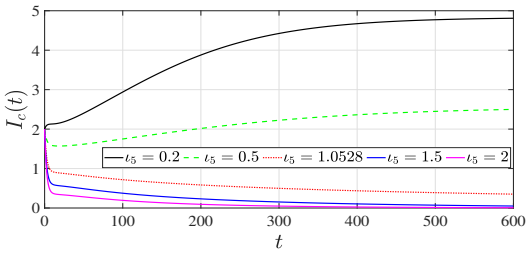


**(g)** Infected copepods in the environment.

**Figure 8.** Disease dynamics under varying environmental development delays $\iota_5$. Longer delays in larval maturation reduce transmission efficiency, with complete disease elimination achieved when $\iota_5 \geq 1.05$ for the initial values $(800, 100, 60, 700, 60, 150, 2)$.

Table 5 and Figure 8 illustrate the significant impact of the environmental development delay $\iota_5$ on

Guinea worm disease transmission dynamics. This delay represents the time required for Guinea worm larvae to mature into infectious forms within copepods in the aquatic environment. Table 5 shows that as the environmental delay $\iota_5$ increases from 0.2 to 2 months, the basic reproduction number $\mathscr{R}_0^d(\iota_5)$ decreases substantially from 2.35 to 0.39. Figure 8 visually demonstrates how longer environmental delays lead to slower disease progression and eventual elimination when $\iota_5 \geq 1.05$, highlighting the importance of environmental factors in parasite lifecycle completion.

- The critical threshold occurs at $\iota_5^{cr} \approx 1.05$ months, where $\mathscr{R}_0^d(\iota_5) = 1$. This represents the minimum developmental delay required to achieve natural disease eradication in the absence of other interventions.
- For shorter delays ($\iota_5 < \iota_5^{cr}$), the disease persists as $\mathscr{R}_0^d(\iota_5) > 1$, with faster larval development leading to more rapid transmission cycles.
- For longer delays ($\iota_5 \geq \iota_5^{cr}$), the disease-free equilibrium becomes globally stable, as extended development times increase larval mortality and reduce successful transmission.

These findings emphasize that environmental conditions affecting larval development time can serve as natural control mechanisms, with longer development periods effectively suppressing disease transmission even without additional interventions.

## 6. Conclusions

This study has developed and analyzed a comprehensive two-patch delayed mathematical model for Guinea worm disease (GWD) dynamics in heterogeneous populations sharing a common water source. Our analysis demonstrates that the basic reproduction number $\mathscr{R}_0^d$ serves as a critical threshold: The disease-free equilibrium is globally asymptotically stable when $\mathscr{R}_0^d \leq 1$, while a unique endemic equilibrium exists and is globally stable when $\mathscr{R}_0^d > 1$. The incorporation of five discrete delays accurately captures key biological time lags in the parasite's lifecycle, including latent periods in humans, maturation within hosts, and environmental development in copepods.

The delay thresholds identified provide important insights into the Guinea worm's lifecycle. The environmental development delay $\iota_5$ has a critical threshold of approximately $\iota_5^{cr} \approx 1.05$ months, revealing a natural vulnerability in the parasite's transmission chain. When environmental conditions prolong this developmental period beyond this threshold, larval mortality increases sharply, suppressing transmission. This suggests that seasonal temperature variations could naturally modulate outbreak risk. Furthermore, the dual representation of latency using both exposed compartments and discrete delays reveals that stage-specific mortality during the incubation period significantly impacts transmission potential, highlighting that interventions targeting host survival during these vulnerable periods could reduce transmission even before clinical symptoms appear.

Our findings offer several actionable recommendations. The critical treatment threshold $\kappa^{cr} = 1 - 1/\mathscr{R}_0^d$ provides a quantitative benchmark: For $\mathscr{R}_0^d = 2.59$, control measures must achieve at least 61% effectiveness to guarantee eradication. Sensitivity analysis identified the pathogen decay rate $\varepsilon$ as the most influential parameter (index $-1$), strongly supporting continued larvicide application and safe water provision. The coupling mechanism through the shared water source $I_c$ implies that interventions benefiting one community indirectly protect the other; conversely, unilateral action may fail if the water source remains contaminated. Thus, coordinated community participation is essential.

Several limitations should be acknowledged. The model assumes constant parameters, while seasonal variations affect transmission. The two-patch structure simplifies complex community networks. Spatial dynamics, migration, and homogeneous mixing assumptions may not fully represent real populations. Additionally, dog populations (important zoonotic reservoirs in Chad) are not included, and parameter values are illustrative due to scarce field data. Promising future directions include incorporating seasonal forcing, extending to multi-patch or network models, integrating optimal control theory, adding spatial components and dog populations, coupling with economic analysis for cost-effectiveness, and validating with longitudinal data from endemic regions.

This study provides a robust mathematical framework for understanding GWD dynamics and offers quantitatively grounded guidance for control strategies. The critical thresholds identified—$\kappa^{cr}$ for treatment efficacy and $\iota_5^{cr}$ for environmental delay—give public health officials specific targets rather than vague recommendations. The sensitivity analysis highlights where resources should be concentrated (larval source management, safe water provision), and the coupling mechanism underscores the necessity of coordinated community action. These insights contribute to the global effort to eradicate this debilitating disease, bringing us closer to the goal of a world free from Guinea worm disease.

## Author contributions

All authors make equal contributions to the research work. All authors have read and agreed to the published version of the manuscript.

## Use of Generative-AI tools declaration

The authors declare they have not used Artificial Intelligence (AI) tools in the creation of this article.

## Acknowledgments

The authors are thankful to the Deanship of Graduate Studies and Scientific Research at Najran University for funding this work under the Consortium Funding Program grant code (NU/CPL/SERC/14/2821-2). The authors would also like to thank the anonymous referees for many constructive suggestions, which helped to improve the presentation of the paper.

## Funding

This work was funded by the Deanship of Graduate Studies and Scientific Research at Najran University under the Najran Research Funding Program-Grant code NU/CPL/SERC/14/2821-2).

## Conflict of interest

All the authors declare there are no conflicts of interest.

## References


1. H. B. Beyene, A. Bekele, A. Shifara, Y. A. Ebstie, Z. Desalegn, Z. Kebede, et al., Elimination of Guinea worm disease in Ethiopia; current status of the Disease's, eradication strategies and challenges to the end game, *Ethiopian Med. J.*, **55** (2017), 15–31.
2. D. Molyneux, D. P. Sankara, Guinea worm eradication: Progress and challenges—should we beware of the dog?, *PLoS Neglect. Trop. D.*, **11** (2017), e0005495. https://doi.org/10.1371/journal.pntd.0005495
3. L. Mari, M. Ciddio, R. Casagrandi, J. P. Saez, E. Bertuzzo, A. Rinaldo, et al., Heterogeneity in schistosomiasis transmission dynamics, *J. Theor. Biol.*, **432** (2017), 87–99. https://doi.org/10.1016/j.jtbi.2017.08.015
4. Water.org, 2026. Available from: `https://water.org/our-impact/where-we-work/`.
5. M. Cheesbrough, S. Curtis, *District laboratory practice in tropical countries*, Cambridge: Cambridge University Press, **53** (2013).
6. G. Biswas, D. P. Sankara, J. Agua-Agum, A. Maiga, Dracuncullasis (guinea worm disease): Eradication without a drug or a vaccine, *Philos. T. Roy. Soc. B*, **368** (2013), 20120146. https://doi.org/10.1098/rstb.2012.0146
7. D. R. Hopkins, E. R. Tiben, T. K. Ruebush, N. Diallo, A. Agle, C. J. Withers, Dracuncullasis eradication: Delayed, not denied, *Am. J. Trop. Med. Hyg.*, **62** (2000), 163–168. https://doi.org/10.4269/ajtmh.2000.62.163
8. V. A. Ilegbodu, O. O. Kale, R. A. Wise, B. L. Christensen, J. H. Steele, L. A. Chambers, Impact of guinea worm disease on children in Nigeria, *Am. J. Trop. Med. Hyg.*, **35** (1986), 962–964.
9. O. P. Lolika, C. Modnak, S. Mushayabasa, On the dynamics of brucellosis infection in bison population with vertical transmission and culling, *Math. Biosci.*, **305** (2018), 42–54. https://doi.org/10.1016/j.mbs.2018.08.009
10. R. Metshikweta, W. Garira, A multiscale model for the world's first parasitic disease targeted for eradication: Guinea worm disease, *Comput. Math. Method. M.*, **2017** (2017), 1473287. https://doi.org/10.1155/2017/1473287
11. N. A. Almuallem, M. E. Hajji, Global dynamics of a multi-population water pollutant model with distributed delays, *Mathematics*, **14** (2026), 20. https://doi.org/10.3390/math14010020
12. F. K. Alalhareth, A. R. Aljohani, M. H. Alharbi, M. E. Hajji, Modeling, stability analysis, and optimal control of a chemostat model for mutualistic bacterial species with leachate recycling, *AIMS Math.*, **10** (2025), 28714–28752. https://doi.org/10.3934/math.20251264
13. A. Lutambi, M. Penny, T. Smith, N. Chitnis, Mathematical modelling of mosquito dispersal in a heterogeneous environment, *Math. Biosci.*, **241** (2013), 198–216. https://doi.org/10.1016/j.mbs.2012.11.013
14. M. E. Hajji, M. F. S. Aloufi, M. H. Alharbi, Influence of seasonality on *Zika* virus transmission, *AIMS Math.*, **9** (2024), 19361–19384. https://doi.org/10.3934/math.2024943
15. F. K. Alalhareth, F. K. Alghamdi, M. H. Alharbi, M. El Hajji, Global dynamics and optimal control of a dual-target hiv model with latent reservoirs, *Mathematics*, **13** (2025), 3868. https://doi.org/10.3390/math13233868

16. I. A. Adetunde, The Epidemiology of guinea worm infection in tamale district, in the northern region of ghana, *J. Mod. Math. Stat.*, 2008, 50–54.
17. R. J. Smith, P. Cloutier, J. Harrison, A. Desforges, *A mathematical model for the eradication of guinea worm disease*, In: Understanding the dynamics of emerging and re-emerging infectious diseases using mathematical models, Transworld Research Network, Kerala, 2012, 133–156.
18. A. E. Losio, S. Mushayabasa, Modeling the effects of spatial heterogeneity and seasonality on guinea worm disease transmission, *J. Appl. Math.*, **2018** (2018), 5084687. https://doi.org/10.1155/2018/5084687
19. X. Y. Meng, X. Z. Sun, Dynamics of a stage-structure diffusive predator–prey model with nonlinear prey refuge, delay and anti-predator behavior, *Int. J. Appl. Comput. Math.*, **12** (2026), 2. https://doi.org/10.1007/s40819-025-02077-4
20. X. Y. Meng, Z. W. Liang, Dynamics analysis of a delayed diffusive predator–prey model with memory-based diffusion and fear effect of prey, *Int. J. Biomath.*, 2025, 2550101. https://doi.org/10.1142/S1793524525501013
21. S. Samanta, S. Rana, A. Sharma, A. K. Misra, J. Chattopadhyay, Effect of awareness programs by media on the epidemic outbreaks: A mathematical model, *Appl. Math. Comput.*, **219** (2013), 6965–6977. https://doi.org/10.1016/j.amc.2013.01.009
22. S. Mushayabasa, C. P. Binnu, R. J. Smith, Assessing the impact of educational campaigns on controlling HCV among women in prison settings, *Commun. Nonlinear Sci.*, **17** (2011), 1714–1724. https://doi.org/10.1016/j.cnsns.2011.08.024
23. A. Sharma, A. K. Misra, Modeling the impact of awareness created by media campaigns on vaccination coverage in a variable population, *J. Biol. Syst.*, **22** (2014), 249–270. https://doi.org/10.1142/S0218339014400051
24. H. R. Joshi, S. Lenhart, S. Hota, F. Agusto, Optimal control of an SIR model with changing behavior through an education campaign, *Electron. J. Differ. Eq.*, **2015** (2015), 1–14.
25. R. Netshikweta, W. Garira, A multiscale model for the world's first parasitic disease targeted for eradication: Guinea worm disease, *Comput. Math. Method. M.*, **2017** (2017), 1473287. https://doi.org/10.1155/2017/1473287
26. M. Helikumi, S. Mushayabasa, Dog screening as a novel complementary guinea worm disease control tool to mitigate persistence in chad: A modeling study, *Parasite Epidem. Cont.*, **23** (2023), e00328. https://doi.org/10.1016/j.parepi.2023.e00328
27. S. Mushayabasa, A. A. E. Losio, C. Modnak, J. Wang, Optimal control analysis applied to a two-patch model for guinea worm disease, *Electron. J. Differ. Eq.*, **2020** (2020), 1–23.
28. E. Lusekelo, S. Daudi, M. Helikumi, S. Mushayabasa, Modeling the implications of seasonality and heterogeneous mean worm burden in guinea-worm disease dynamics in dog population, *Nonlin. Sci.*, **4** (2025), 100031. https://doi.org/10.1016/j.nls.2025.100031
29. H. Smalley, P. Keskinocak, J. Swann, C. Hanna, A. Weiss, Proactive tethering to prevent guinea worm infections among dogs in chad: An analysis of the impacts of timing and dog selection, *Am. J. Trop. Med. Hyg.*, **113** (2025), 317–323. https://doi.org/10.4269/ajtmh.24-0673
30. O. O. Alew, N. Peters, Ethiopian dracuncullasis eradication program (EDEP) GOG WOREDA meeting, *National Rev.*, 2015, 14–15.

31. P. V. den Driessche, J. Watmough, Reproduction numbers and sub-threshold endemic equilibria for compartmental models of disease transmission, *Math. Biosci.*, **180** (2002), 29–48. https://doi.org/10.1016/S0025-5564(02)00108-6
32. J. P. LaSalle, *The stability of dynamical systems*, Philadelphia: SIAM, 1976.
33. M. E. Hajji, Y. A. Al-Faidi, M. H. Alharbi, Modeling dual-colony nosema transmission in honeybees: The role of distributed delays and antiviral treatment, *AIMS Math.*, **11** (2026), 2645–2681. https://doi.org/10.3934/math.2026107
34. H. H. Almuashi, M. E. Hajji, Global dynamics of a dual-target HIV model with time delays and treatment implications, *Mathematics*, **14** (2026), 6. https://doi.org/10.3390/math14010006
35. N. Chitnis, J. M. Hyman, J. M. Cushing, Determining important parameters in the spread of malaria through the sensitivity analysis of a mathematical model, *B. Math. Biol.*, **70** (2008), 1272–1296. https://doi.org/10.1007/s11538-008-9299-0
36. J. K. Hale, A. S. Somolinos, Competition for a fluctuating nutrient, *J. Math. Biol.*, **18** (1983), 255–280. https://doi.org/10.1007/BF00276091
37. H. Khalil, *Nonlinear systems*, 2 Eds., Prentice Hall, 1996.


## A. Proof of Theorems 5 and 6

### *A.1. Proof of Theorem 5*

*Proof of Theorem 5.* Let us consider a candidate Lyapunov function $\mathscr{F}_0^d(S_1,E_1,I_1,S_2,E_2,I_2,I_c)$ given by

$$\begin{aligned}\mathscr{F}_0^d &= F_1F_2F_5\frac{S_1^{in}}{d_1}\Phi\left(\frac{d_1S_1}{S_1^{in}}\right)+F_2F_5E_1+F_5\frac{d_1+\sigma_1}{\sigma_1}I_1+F_3F_4F_5\frac{d_1p_2\sigma_2(d_1+\sigma_1)}{d_2p_1\sigma_1(d_2+\sigma_2)}\frac{S_2^{in}}{d_2}\Phi\left(\frac{d_2S_2}{S_2^{in}}\right)\\
&+F_4F_5\frac{d_1p_2\sigma_2(d_1+\sigma_1)}{d_2p_1\sigma_1(d_2+\sigma_2)}E_2+F_5\frac{d_1p_2(d_1+\sigma_1)}{d_2p_1\sigma_1}I_2+\frac{d_1(d_1+\sigma_1)}{p_1\sigma_1}I_c+F_1F_2F_5\beta_1\int_{t-\iota_1}^{t}S_1(\theta)I_c(\theta)d\theta\\
&+F_2F_5(d_1+\sigma_1)\int_{t-\iota_2}^{t}E_1(\theta)d\theta+F_3F_4F_5\beta_2\frac{d_1p_2\sigma_2(d_1+\sigma_1)}{d_2p_1\sigma_1(d_2+\sigma_2)}\int_{t-\iota_3}^{t}S_2(\theta)I_c(\theta)d\theta\\
&+F_4F_5\frac{d_1p_2\sigma_2(d_1+\sigma_1)}{d_2p_1\sigma_1}\int_{t-\iota_4}^{t}E_2(\theta)d\theta+\frac{d_1(d_1+\sigma_1)}{p_1\sigma_1}F_5\int_{t-\iota_5}^{t}\big(p_1I_1(\theta)+p_2I_2(\theta)\big)d\theta.\end{aligned}$$

Calculating $\dfrac{d\mathscr{F}_0^d}{dt}$ along the trajectories of the dynamics (2.1) gives

$$\begin{aligned}\frac{d\mathscr{F}_0^d}{dt} &= F_1F_2F_5\left(1-\frac{S_1^{in}}{d_1S_1}\right)\dot{S}_1+F_2F_5\dot{E}_1+F_5\frac{d_1+\sigma_1}{\sigma_1}\dot{I}_1+F_3F_4F_5\frac{d_1p_2\sigma_2(d_1+\sigma_1)}{d_2p_1\sigma_1(d_2+\sigma_2)}\left(1-\frac{S_2^{in}}{d_2S_2}\right)\dot{S}_2\\
&+F_4F_5\frac{d_1p_2\sigma_2(d_1+\sigma_1)}{d_2p_1\sigma_1(d_2+\sigma_2)}\dot{E}_2+F_5\frac{d_1p_2(d_1+\sigma_1)}{d_2p_1\sigma_1}\dot{I}_2+\frac{d_1(d_1+\sigma_1)}{p_1\sigma_1}\dot{I}_c\\
&+F_1F_2F_5\beta_1(S_1I_c-S_1(t-\iota_1)I_c(t-\iota_1))+F_2F_5(d_1+\sigma_1)(E_1-E_1(t-\iota_2))\\
&+F_3F_4F_5\beta_2\frac{d_1p_2\sigma_2(d_1+\sigma_1)}{d_2p_1\sigma_1(d_2+\sigma_2)}(S_2I_c-S_2(t-\iota_3)I_c(t-\iota_3))+F_4F_5\frac{d_1p_2\sigma_2(d_1+\sigma_1)}{d_2p_1\sigma_1}(E_2-E_2(t-\iota_4))\\
&+F_5\frac{d_1(d_1+\sigma_1)}{p_1\sigma_1}\big[p_1(I_1-I_1(t-\iota_5))+p_2(I_2-I_2(t-\iota_5))\big].\end{aligned}$$

From dynamics (2.1), we get

$$\begin{aligned}\frac{d\mathscr{F}_0^d}{dt} &= -F_1F_2F_5\frac{d_1}{S_1}\left(S_1-\frac{S_1^{in}}{d_1}\right)^2 - F_1F_2F_5\beta_1S_1I_c + F_1F_2F_5\beta_1\frac{S_1^{in}}{d_1}I_c - F_2F_5(d_1+\sigma_1)E_1\\ &\quad -F_5\frac{(d_1+\sigma_1)}{\sigma_1}d_1I_1 - F_3F_4F_5\frac{d_1p_2\sigma_2(d_1+\sigma_1)}{S_2p_1\sigma_1(d_2+\sigma_2)}\left(S_2-\frac{S_2^{in}}{d_2}\right)^2\\ &\quad -F_3F_4F_5\frac{d_1p_2\sigma_2(d_1+\sigma_1)}{d_2p_1\sigma_1(d_2+\sigma_2)}\beta_2S_2I_c + F_3F_4F_5\frac{d_1p_2\sigma_2(d_1+\sigma_1)}{d_2p_1\sigma_1(d_2+\sigma_2)}\beta_2\frac{S_2^{in}}{d_2}I_c\\ &\quad -F_4F_5\frac{d_1p_2\sigma_2(d_1+\sigma_1)}{d_2p_1\sigma_1}E_2 - F_5\frac{d_1p_2(d_1+\sigma_1)}{d_2p_1\sigma_1}d_2I_2 - \frac{d_1(d_1+\sigma_1)}{p_1\sigma_1}\varepsilon I_c\\ &\quad +F_1F_2F_5\beta_1S_1I_c + F_2F_5(d_1+\sigma_1)E_1 + F_3F_4F_5\frac{d_1p_2\sigma_2(d_1+\sigma_1)}{d_2p_1\sigma_1(d_2+\sigma_2)}\beta_2S_2I_c\\ &\quad +F_4F_5\frac{d_1p_2\sigma_2(d_1+\sigma_1)}{d_2p_1\sigma_1}E_2 + F_5\frac{d_1(d_1+\sigma_1)}{p_1\sigma_1}\left[p_1I_1+p_2I_2\right].\end{aligned}$$

Collecting terms, we obtain

$$\begin{aligned}\frac{d\mathscr{F}_0^d}{dt} &= -F_1F_2F_5\frac{d_1}{S_1}\left(S_1-\frac{S_1^{in}}{d_1}\right)^2 - F_3F_4F_5\frac{d_1p_2\sigma_2(d_1+\sigma_1)}{S_2p_1\sigma_1(d_2+\sigma_2)}\left(S_2-\frac{S_2^{in}}{d_2}\right)^2\\ &\quad +\frac{\varepsilon d_1(d_1+\sigma_1)}{p_1\sigma_1}\left(\frac{p_1\sigma_1\beta_1F_1F_2F_5S_1^{in}}{\varepsilon d_1^2(d_1+\sigma_1)} + \frac{p_2\sigma_2\beta_2F_3F_4F_5S_2^{in}}{\varepsilon d_2^2(d_2+\sigma_2)} - 1\right)I_c.\end{aligned}$$

Finally, we obtain

$$\frac{d\mathscr{F}_0^d}{dt} = -F_1F_2F_5\frac{d_1}{S_1}\left(S_1-\frac{S_1^{in}}{d_1}\right)^2 - F_3F_4F_5\frac{d_1p_2\sigma_2(d_1+\sigma_1)}{S_2p_1\sigma_1(d_2+\sigma_2)}\left(S_2-\frac{S_2^{in}}{d_2}\right)^2 + \frac{\varepsilon d_1(d_1+\sigma_1)}{p_1\sigma_1}\left(\mathscr{R}_0^d-1\right)I_c.$$

Therefore, for all $S_1,E_1,I_1,S_2,E_2,I_2,I_c>0$ we have $\frac{d\mathscr{F}_0^d}{dt}\leq 0$ when $\mathscr{R}_0^d\leq 1$. Moreover, $\frac{d\mathscr{F}_0^d}{dt}=0$ when $S_1=\frac{S_1^{in}}{d_1}$, $S_2=\frac{S_2^{in}}{d_2}$, and $(\mathscr{R}_0^d-1)I_c=0$. According to [36], solutions of system (2.1) limit to the largest invariant subset of $\left\{(S_1,E_1,I_1,S_2,E_2,I_2,I_c):\frac{d\mathscr{F}_0^d}{dt}=0\right\}$, which contains elements with $S_1(t)=\frac{S_1^{in}}{d_1}$, $S_2(t)=\frac{S_2^{in}}{d_2}$, and

$$(\mathscr{R}_0^d-1)I_c=0. \tag{A.1}$$

Let us consider two cases:

- If $\mathscr{R}_0^d<1$, then from Eq (A.1), we obtain $I_c=0$. Since the largest invariant subset of

$$\left\{(S_1,E_1,I_1,S_2,E_2,I_2,I_c):\frac{d\mathscr{F}_0^d}{dt}=0\right\}$$

is invariant, we obtain $\dot{I}_c(t)=0$. Then,

$$0=F_5\left[p_1I_1(t-\iota_5)+p_2I_2(t-\iota_5)\right]\Rightarrow I_1(t)=I_2(t)=0,\forall t. \tag{A.2}$$

Furthermore, since $I_1 = 0$, then $\dot{I}_1(t) = \sigma_1 F - 2E_1(t-\iota_2) = 0$, and thus $E_1(t) = 0$, for any $t$. By the same approach, $I_2 = 0$, so then $\dot{I}_2(t) = \sigma_2 F_4 E_2(t-\iota_4) = 0$, and thus $E_2(t) = 0$ for any $t$. Hence, the largest invariant subset of $\left\{(S_1, E_1, I_1, S_2, E_2, I_2, I_c) : \dfrac{d\mathscr{F}_0^d}{dt} = 0\right\} = \left\{\mathscr{E}_0^d\right\}$.

- If $\mathscr{R}_0^d = 1$, we have $S_1 = \dfrac{S_1^{in}}{d_1}$, $S_2 = \dfrac{S_2^{in}}{d_2}$, then $\dot{S}_1(t) = \dot{S}_2(t) = 0$. From (2.1), we have

$$S_2^{in} - S_2^{in} - \beta_2 \frac{S_2^{in}}{d_2} I_c = 0 \Longrightarrow I_c(t) = 0, \forall t. \tag{A.3}$$

According to (A.2), we deduce that $I_1(t) = I_2(t) = E_1(t) = E_2(t) = 0$ for all $t \geq 0$. Hence, the largest invariant subset of $\left\{(S_1, E_1, I_1, S_2, E_2, I_2, I_c) : \dfrac{d\mathscr{F}_0^d}{dt} = 0\right\} = \left\{\mathscr{E}_0^d\right\}$.

By applying LaSalle's invariance principle [37], we conclude that $\mathscr{E}_0^d = \left(\dfrac{S_1^{in}}{d_1}, 0, 0, \dfrac{S_2^{in}}{d_2}, 0, 0, 0\right)$ is GAS once $\mathscr{R}_0^d \leq 1$. □

*A.2. Proof of Theorem 6*

*Proof of Theorem 6.* Let us define a candidate Lyapunov function $\mathscr{F}_d^*(S_1, E_1, I_1, S_2, E_2, I_2, I_c)$:

$$\begin{aligned}
\mathscr{F}_d^* \;=\; & F_1F_2F_5S_1^*\Phi\left(\frac{S_1}{S_1^*}\right) + F_2F_5E_1^*\Phi\left(\frac{E_1}{E_1^*}\right) + F_5\frac{d_1+\sigma_1}{\sigma_1}I_1^*\Phi\left(\frac{I_1}{I_1^*}\right) \\
& + F_3F_4F_5\frac{d_1p_2\sigma_2(d_1+\sigma_1)}{d_2p_1\sigma_1(d_2+\sigma_2)}S_2^*\Phi\left(\frac{S_2}{S_2^*}\right) + F_4F_5\frac{d_1p_2\sigma_2(d_1+\sigma_1)}{d_2p_1\sigma_1(d_2+\sigma_2)}E_2^*\Phi\left(\frac{E_2}{E_2^*}\right) \\
& + F_5\frac{d_1p_2(d_1+\sigma_1)}{d_2p_1\sigma_1}I_2^*\Phi\left(\frac{I_2}{I_2^*}\right) + \frac{d_1(d_1+\sigma_1)}{p_1\sigma_1}I_c^*\Phi\left(\frac{I_c}{I_c^*}\right) \\
& + F_1F_2F_5\beta_1S_1^*I_c^*\int_{t-\iota_1}^{t}\Phi\left(\frac{S_1(\theta)I_c(\theta)}{S_1^*I_c^*}\right)d\theta \\
& + F_2F_5(d_1+\sigma_1)E_1^*\int_{t-\iota_2}^{t}\Phi\left(\frac{E_1(\theta)}{E_1^*}\right)d\theta \\
& + F_3F_4F_5\beta_2\frac{d_1p_2\sigma_2(d_1+\sigma_1)}{d_2p_1\sigma_1(d_2+\sigma_2)}S_2^*I_c^*\int_{t-\iota_3}^{t}\Phi\left(\frac{S_2(\theta)I_c(\theta)}{S_2^*I_c^*}\right)d\theta \\
& + F_4F_5\frac{d_1p_2\sigma_2(d_1+\sigma_1)}{d_2p_1\sigma_1}E_2^*\int_{t-\iota_4}^{t}\Phi\left(\frac{E_2(\theta)}{E_2^*}\right)d\theta \\
& + F_5\frac{d_1(d_1+\sigma_1)}{p_1\sigma_1}\int_{t-\iota_5}^{t}\left(p_1I_1^*\Phi\left(\frac{I_1(\theta)}{I_1^*}\right) + p_2I_2^*\Phi\left(\frac{I_2(\theta)}{I_2^*}\right)\right)d\theta.
\end{aligned}$$

By calculating $\dfrac{d\mathscr{F}_d^*}{dt}$ along the trajectories of dynamics (2.1), we get

$$
\begin{aligned}
\frac{d\mathscr{F}_d^*}{dt} &= F_1F_2F_5\left(1-\frac{S_1^*}{S_1}\right)\left(S_1^{in}-d_1S_1-\beta_1S_1I_c\right)\\
&+F_2F_5\left(1-\frac{E_1^*}{E_1}\right)\left(\beta_1F_1S_1(t-\iota_1)I_c(t-\iota_1)-(d_1+\sigma_1)E_1\right)\\
&+F_5\frac{d_1+\sigma_1}{\sigma_1}\left(1-\frac{I_1^*}{I_1}\right)\left(\sigma_1F_2E_1(t-\iota_2)-d_1I_1\right)\\
&+F_3F_4F_5\frac{d_1p_2\sigma_2(d_1+\sigma_1)}{d_2p_1\sigma_1(d_2+\sigma_2)}\left(1-\frac{S_2^*}{S_2}\right)\left(S_2^{in}-d_2S_2-\beta_2S_2I_c\right)\\
&+F_4F_5\frac{d_1p_2\sigma_2(d_1+\sigma_1)}{d_2p_1\sigma_1(d_2+\sigma_2)}\left(1-\frac{E_2^*}{E_2}\right)\left(\beta_2F_3S_2(t-\iota_3)I_c(t-\iota_3)-(d_2+\sigma_2)E_2\right)\\
&+F_5\frac{d_1p_2(d_1+\sigma_1)}{d_2p_1\sigma_1}\left(1-\frac{I_2^*}{I_2}\right)\left(\sigma_2F_4E_2(t-\iota_4)-d_2I_2\right)\\
&+\frac{d_1(d_1+\sigma_1)}{p_1\sigma_1}\left(1-\frac{I_c^*}{I_c}\right)\left(F_5\left[p_1I_1(t-\iota_5)+p_2I_2(t-\iota_5)\right]-\varepsilon I_c\right)\\
&+F_1F_2F_5\beta_1S_1^*I_c^*\left[\frac{S_1I_c}{S_1^*I_c^*}-\frac{S_1(t-\iota_1)I_c(t-\iota_1)}{S_1^*I_c^*}+\ln\left(\frac{S_1(t-\iota_1)I_c(t-\iota_1)}{S_1I_c}\right)\right]\\
&+F_2F_5(d_1+\sigma_1)E_1^*\left[\frac{E_1}{E_1^*}-\frac{E_1(t-\iota_2)}{E_1^*}+\ln\left(\frac{E_1(t-\iota_2)}{E_1}\right)\right]\\
&+F_3F_4F_5\beta_2\frac{d_1p_2\sigma_2(d_1+\sigma_1)}{d_2p_1\sigma_1(d_2+\sigma_2)}S_2^*I_c^*\left[\frac{S_2I_c}{S_2^*I_c^*}-\frac{S_2(t-\iota_3)I_c(t-\iota_3)}{S_2^*I_c^*}+\ln\left(\frac{S_2(t-\iota_3)I_c(t-\iota_3)}{S_2I_c}\right)\right]\\
&+F_4F_5\frac{d_1p_2\sigma_2(d_1+\sigma_1)}{d_2p_1\sigma_1}E_2^*\left[\frac{E_2}{E_2^*}-\frac{E_2(t-\iota_4)}{E_2^*}+\ln\left(\frac{E_2(t-\iota_4)}{E_2}\right)\right]
\end{aligned}
$$

$$
+F_5\frac{d_1(d_1+\sigma_1)}{p_1\sigma_1}\left(p_1I_1^*\left[\frac{I_1}{I_1^*}-\frac{I_1(t-\iota_5)}{I_1^*}+\ln\left(\frac{I_1(t-\iota_5)}{I_1}\right)\right]+p_2I_2^*\left[\frac{I_2}{I_2^*}-\frac{I_2(t-\iota_5)}{I_2^*}+\ln\left(\frac{I_2(t-\iota_5)}{I_2}\right)\right]\right).
$$

By using the equilibrium conditions

$$
\begin{aligned}
&S_1^{in}=d_1S_1^*+\beta_1S_1^*I_c^*,\ d_2S_2^{in}=d_2S_2^*+\beta_2S_2^*I_c^*,\ F_5(p_1I_1^*+p_2I_2^*)=\varepsilon I_c^*,\\
&\beta_1F_1S_1^*I_c^*=(d_1+\sigma_1)E_1^*,\sigma_1F_2E_1^*=d_1I_1^*,\ \beta_2F_3S_2^*I_c^*=(d_2+\sigma_2)E_2^*,\sigma_2F_4E_2^*=d_2I_2^*,
\end{aligned}
$$

we get $d_1I_1^*=\sigma_1F_2E_1^*=\dfrac{\sigma_1F_1F_2}{(d_1+\sigma_1)}\beta_1S_1^*I_c^*,d_2I_2^*=\sigma_2F_4E_2^*=\dfrac{\sigma_2F_3F_4}{(d_2+\sigma_2)}\beta_2S_2^*I_c^*,$ and

$$
\begin{aligned}
\frac{d\mathscr{F}_d^*}{dt} &= -F_1F_2F_5\frac{d_1(S_1-S_1^*)^2}{S_1}-F_3F_4F_5\frac{d_1p_2\sigma_2(d_1+\sigma_1)}{d_2p_1\sigma_1(d_2+\sigma_2)}\frac{d_2(S_2-S_2^*)^2}{S_2}\\
&+F_1F_2F_5\beta_1S_1^*I_c^*\left(1-\frac{S_1^*}{S_1}\right)+F_3F_4F_5\frac{d_1p_2\sigma_2(d_1+\sigma_1)}{d_2p_1\sigma_1(d_2+\sigma_2)}\beta_2S_2^*I_c^*\left(1-\frac{S_2^*}{S_2}\right)\\
&+F_1F_2F_5\beta_1S_1^*I_c^*\left[1-\frac{S_1(t-\iota_1)I_c(t-\iota_1)E_1^*}{S_1^*I_c^*E_1}+\ln\left(\frac{S_1(t-\iota_1)I_c(t-\iota_1)}{S_1I_c}\right)\right]\\
&+F_1F_2F_5\beta_1S_1^*I_c^*\left[1-\frac{E_1(t-\iota_2)I_1^*}{E_1^*I_1}+\ln\left(\frac{E_1(t-\iota_2)}{E_1}\right)\right]\\
&+F_3F_4F_5\frac{d_1p_2\sigma_2(d_1+\sigma_1)}{d_2p_1\sigma_1(d_2+\sigma_2)}\beta_2S_2^*I_c^*\left[1-\frac{S_2(t-\iota_3)I_c(t-\iota_3)E_2^*}{S_2^*I_c^*E_2}+\ln\left(\frac{S_2(t-\iota_3)I_c(t-\iota_3)}{S_2I_c}\right)\right]\\
&+F_3F_4F_5\frac{d_1p_2\sigma_2(d_1+\sigma_1)}{d_2p_1\sigma_1(d_2+\sigma_2)}\beta_2S_2^*I_c^*\left[1-\frac{E_2(t-\iota_4)I_2^*}{E_2^*I_2}+\ln\left(\frac{E_2(t-\iota_4)}{E_2}\right)\right]\\
&+F_1F_2F_5\beta_1S_1^*I_c^*\left[1-\frac{I_1^tI_c^*}{I_1^*I_c}+\ln\left(\frac{I_1(t-\iota_5)}{I_1}\right)\right]\\
&+F_3F_4F_5\frac{d_1p_2\sigma_2(d_1+\sigma_1)}{d_2p_1\sigma_1(d_2+\sigma_2)}\beta_2S_2^*I_c^*\left[1-\frac{I_2(t-\iota_5)I_c^*}{I_2^*I_c}+\ln\left(\frac{I_2(t-\iota_5)}{I_2}\right)\right].
\end{aligned}
$$

Applying the following equalities:

$$\ln\left(\frac{S_1(t-\iota_1)I_c(t-\iota_1)}{S_1I_c}\right)+\ln\left(\frac{E_1(t-\iota_2)}{E_1}\right)+\ln\left(\frac{I_1(t-\iota_5)}{I_1}\right)=$$
$$\ln\left(\frac{S_1^*}{S_1}\right)+\ln\left(\frac{S_1(t-\iota_1)I_c(t-\iota_1)E_1^*}{S_1^*I_c^*E_1}\right)+\ln\left(\frac{E_1(t-\iota_2)I_1^*}{E_1^*I_1}\right)+\ln\left(\frac{I_1(t-\iota_5)I_c^*}{I_1^*I_c}\right),$$
$$\ln\left(\frac{S_2(t-\iota_3)I_c(t-\iota_3)}{S_2I_c}\right)+\ln\left(\frac{E_2(t-\iota_4)}{E_2}\right)+\ln\left(\frac{I_2(t-\iota_5)}{I_2}\right)=$$
$$\ln\left(\frac{S_2^*}{S_2}\right)+\ln\left(\frac{S_2(t-\iota_3)I_c(t-\iota_3)E_2^*}{S_2^*I_c^*E_2}\right)+\ln\left(\frac{E_2(t-\iota_4)I_2^*}{E_2^*I_2}\right)+\ln\left(\frac{I_2(t-\iota_5)I_c^*}{I_2^*I_c}\right),$$

we obtain

$$\begin{aligned}\frac{d\mathscr{F}_d^*}{dt} &= -F_1F_2F_5\frac{d_1(S_1-S_1^*)^2}{S_1}-F_3F_4F_5\frac{d_1p_2\sigma_2(d_1+\sigma_1)}{d_2p_1\sigma_1(d_2+\sigma_2)}\frac{d_2(S_2-S_2^*)^2}{S_2}-F_1F_2F_5\beta_1S_1^*I_c^*\Phi\left(\frac{S_1^*}{S_1}\right)\\ &\quad -F_3F_4F_5\frac{d_1p_2\sigma_2(d_1+\sigma_1)}{d_2p_1\sigma_1(d_2+\sigma_2)}\beta_2S_2^*I_c^*\Phi\left(\frac{S_2^*}{S_2}\right)-F_1F_2F_5\beta_1S_1^*I_c^*\Phi\left(\frac{S_1(t-\iota_1)I_c(t-\iota_1)}{S_1^*I_c^*}\frac{E_1^*}{E_1}\right)\\ &\quad -F_1F_2F_5\beta_1S_1^*I_c^*\Phi\left(\frac{I_1^*}{I_1}\frac{E_1(t-\iota_2)}{E_1^*}\right)-F_3F_4F_5\frac{d_1p_2\sigma_2(d_1+\sigma_1)}{d_2p_1\sigma_1(d_2+\sigma_2)}\beta_2S_2^*I_c^*\Phi\left(\frac{S_2(t-\iota_3)I_c(t-\iota_3)}{S_2^*I_c^*}\frac{E_2^*}{E_2}\right)\\ &\quad -F_3F_4F_5\frac{d_1p_2\sigma_2(d_1+\sigma_1)}{d_2p_1\sigma_1(d_2+\sigma_2)}\beta_2S_2^*I_c^*\Phi\left(\frac{E_2(t-\iota_4)}{E_2^*}\frac{I_2^*}{I_2}\right)-F_1F_2F_5\beta_1S_1^*I_c^*\Phi\left(\frac{I_1(t-\iota_5)}{I_1^*}\frac{I_c^*}{I_c}\right)\\ &\quad -F_3F_4F_5\frac{d_1p_2\sigma_2(d_1+\sigma_1)}{d_2p_1\sigma_1(d_2+\sigma_2)}\beta_2S_2^*I_c^*\Phi\left(\frac{I_2(t-\iota_5)}{I_2^*}\frac{I_c^*}{I_c}\right).\end{aligned}$$

Therefore, $\frac{d\mathscr{F}_d^*}{dt}\leq 0$. Furthermore, $\frac{d\mathscr{F}_d^*}{dt}=0$ exactly if $(S_1,E_1,I_1,S_2,E_2,I_2,I_c)=(S_1^*,E_1^*,I_1^*,S_2^*,E_2^*,I_2^*,I_c^*)$. By using LaSalle's invariance principle, we deduce that $\mathscr{E}_d^*$ is GAS once $\mathscr{R}_0^d>1$. □